LAWRENCE
LIVERMORE
NATIONAL
LABORATORY

UCRL-TR-219647

Compaction of Expancel Microspheres and Epoxy Foam to 3 GPa

S. R. Carlson, B. P. Bonner, F. J. Ryerson, C. T. S. Chow

March 8, 2006

This work was performed under the auspices of the U.S. Department of Energy by University of California, Lawrence Livermore National Laboratory under Contract W-7405-Eng-48.

List of Figures

List of Tables

Compaction of Expancel Microspheres and Epoxy Foam to 3 GPa

Steven R. Carlson, Brian P. Bonner, Fredrick J. Ryerson and Charles T. S. Chow
Lawrence Livermore National Laboratory
Livermore, California 94551

Abstract

Pressure-volume relationships were measured for unexpanded Expancel microspheres, epoxy foam and one specimen of crushed foam powder. The specimens were jacketed in tin canisters and compressed at ambient temperature and low strain rates to 3 GPa in a solid medium press. Pressures were corrected for friction, and specimen volumes were calculated relative to a nickel standard. The pressure-volume curves for each material show large volume reductions at pressures below 0.1 GPa. The curves stiffen sharply at or near full density. Relatively little volume reduction is observed above 0.1 GPa, and most is recovered on unloading. The energy expended in compressing the materials to 3 GPa and the energy recovered on unloading were determined by numerically integrating the pressure-volume curves. The net energy, which includes absorbed energy, was found to be small. Compressibilities and bulk moduli were determined from the slopes of the pressure-volume curves. The Expancel bulk modulus above 0.1 GPa was found to be similar to that of isopentane. The pressure-volume data were fit to a model from the ceramics literature (Kawakita and Ludde, 1970). The model fits provided estimates of the initial specimen porosities and room pressure bulk moduli.

1. Introduction

This report describes quasi-static pressure-volume measurements for dry, unexpanded Expancel microspheres and epoxy foam specimens. The experimental techniques and data reduction procedures are similar to those employed in earlier studies at LLNL on fractured rocks and other earth materials (Stephens and Lilley, 1966), alluvium (Heard and Stephens, 1970), powders (Weed, 1984) and, more recently, ceramic microspheres and spherical molybdenum powder (Carlson et al. 2005).

The highly porous materials in this study can be expected to undergo large amounts of compaction under hydrostatic pressure. Expancel microspheres consist of thin, thermoplastic shells enclosing gas and a small quantity of liquid isopentane. When heated sufficiently, the isopentane vaporizes and the microspheres inflate until their shells are approximately 0.1 μm thick (Akzo Nobel, 2004). The expanded microspheres have low densities and compress readily at low pressures. Depending on density, a confining pressure of 1 MPa can cause a 20 - 80% volume reduction for expanded Expancel 551 DE 40 microspheres (Akzo Nobel, 2004). The denser, unexpanded microspheres studied here are stiffer, but should also undergo a considerable volume reduction at low

pressures. The epoxy foam consists of a large number of pores of various sizes separated by thin cell walls. The elastic moduli of foams are typically controlled by the bending stiffness of the cell walls; collapse occurs by elastic buckling of the cell walls or by the formation of plastic hinges (Gibson and Ashley, 1982). The collapse of the thin cell walls can be expected to occur at relatively low pressures and to lead to a great reduction in volume. After most pores have collapsed, the material may behave like a powder. With this in mind, one specimen was prepared by manually crushing pieces of foam into a fine powder.

2. Methods

2.1 Material Descriptions

Expancel microspheres are small, hollow spherical particles manufactured by Akzo Nobel and designed to expand dramatically when heated above 100° C. An unexpanded microsphere consists of a thermoplastic shell that encloses a drop of liquid isopentane. On heating the shell softens and the liquid vaporizes, causing the microsphere to expand. Dry, unexpanded microspheres (Expancel 551 DU 40) were selected for compression testing. An SEM photograph of the Expancel microspheres is given in Figure 1. The microspheres are 10-16 μm in diameter and have a bulk density of 0.63 g/cm^3. An apparent grain density, i.e.- the particle density if the microspheres were solid, of 1.137 g/cm^3 was found from helium pycnometer measurements. This value is well within the 1.0–1.2 g/cm^3 density range given by the manufacturer. However, the true grain density may be higher if the microspheres are impermeable to helium. An unsuccessful attempt was made to crush a sample of the microspheres with a mortar and pestle. The porosity of 44-45% calculated from the grain density obtained from the pycnometer data should be considered a lower bound, because pore space within the microspheres may have been missed.

The foam material is an epoxy foam composed of three main components: 1) low viscosity cycloaliphatic epoxy resin. 2) vinyl-4-cyclohexene dioxide. 3) tri-m, p-cresyl borate (Table 1). Pores occur in a wide range of sizes. The foam's outer crust is dense, brittle and rigid. The interior is light yellow in color, soft to the touch and emits an odor similar to creosote. Our specimens were taken from the interior of the foam, which has a bulk density of about 0.20 to 0.24 g/cm^3. A grain density of 1.14 g/cm^3 was obtained from helium pycnometer measurements on two samples of crushed foam (Table 2). The bulk and grain densities yield a porosity of about 80%. This value is somewhat smaller than the 88% porosity obtained by Carlson et al. (2005) for another (different) epoxy foam. A portion of foam was manually ground into a fine powder and a single specimen was prepared. The crushed foam powder specimen has a bulk density of 0.63 g/cm^3 and a porosity of 44.6%. It was noted that the powder particles tended to clump together, probably because of adsorbed moisture. The moisture may have increased the both the mass and the volume of the powder samples slightly, and may impart a small error to the porosity values.

2.2 Specimen Preparation

Three Expancel microsphere specimens were prepared in the same manner as the solid medium test specimens described in Carlson et al. (2005). The jacketed specimens are 12.7 mm in outer diameter and 30.2 mm in length. The microspheres were poured into the canisters in five stages and were vibrated on a Fritsch Analysette 3 sieve shaker for ten minutes after each partial fill. A thin indium (1.6 mm thick) disk and a tin lid of the same dimensions were placed on top of the powder to complete the specimen. The powder depth is 25.4 mm if the canister is filled so that the lid is flush with the jacket rim. Two specimens, Expancel #1 and #2, were found to be slightly under-filled, and a thin ring of tin was trimmed off the jacket wall of each so that the tops of the specimens are flat. As a result, these specimens are slightly shorter than intended. The soft indium disks allow the loading stress to be applied more uniformly to the powder. The lids were not soldered into place, and some air may vent from the specimens at low pressure before the tin flows sufficiently to form a seal. A cylinder of high purity nickel was jacketed in a tin canister in the same manner as the test specimens to serve as a reference standard.

The foam arrived in a one-liter stainless steel bottle labeled 137405. We cut off one end of the bottle with a band saw to expose the foam (Figure 2). The foam did not adhere to the sides of the bottle and was easily removed. The outer surface of the foam cylinder is stiff and dense, but the interior is soft and porous (Figure 3). The brittle outer skin has largely broken off from the top portion of the foam cylinder (Figure 4). Because of its odor, the foam was stored under a fume hood after being removed from the steel bottle. The foam was cut into three sections, each about 48 mm long, labeled A, B, and C (Figure 5a). Three-to-five cores, each 11.7 mm in diameter, were bored by hand with a cork borer from each section. Approximate locations of the cores are shown in Figure 5b. Several cores fell apart or were found to contain one or more very large pores and were rejected as test specimens. The rejected cores were ground into a fine powder with a mortar and pestle. One portion of the crushed foam powder served as a powder specimen, and a second portion was retained for grain density measurements. The foam cores were trimmed to one-inch lengths with a razor blade, and the ends were gently abraded with sandpaper. The foam cylinders were then inserted into tin canisters identical to those used for the Expancel specimens. The foam cores are soft and may have suffered some damage during handling. A thin indium disk was placed on top of foam, followed by a tin lid. One specimen of crushed foam powder was prepared in the same manner as the Expancel microsphere specimens. Because the foam contains some fairly sizeable pores, an attempt was made to fabricate larger specimens having a diameter of 19 mm and a length of 38 mm. However, we were not able to press out good quality tin canisters of this size, and the effort was abandoned.

The various components of each specimen were weighed on a sensitive mass balance and dimensions were measured with a micrometer. The foam cores proved too soft to be measured reliably with a micrometer. Therefore, the initial dimensions of both the foam and the Expancel specimens were calculated from the interior dimensions of the tin canisters, after subtracting the thickness of the indium disks. Bulk densities (Figure 6) were calculated by dividing specimen mass by volume. Grain densities of 1.141 g/cm^3

for the foam and 1.137 g/cm^3 for the Expancel microspheres were obtained by weighing small quantities of these materials on a sensitive mass balance and then measuring powder volumes in a helium pycnometer. The specimen densities and porosities are given in Table 3.

2.3 Experimental Procedures

All of the compression tests were made in the red 400-ton press located in Room 1005 of Building 243. The press consists of a steel reaction frame, a compound die, a tungsten carbide piston and anvil and two hydraulic rams. The larger, 400-ton hydraulic ram lifts the die and smaller Enerpac ram against the reaction frame to provide a clamping load. The Enerpac ram then drives the piston upward through the die bore to compress the specimen against the anvil. Loading is controlled with a PC-PCS Pressure Control System supplied by Rockland Research Corporation. The pressure control system provides a well-controlled, uniform loading rate. A loading rate of 1000 rpm was used in all of the compression tests, except Expancel #2, for which the loading rate was 1500 rpm. The loading rates translate to a piston speed of 1.0 cm/hour per 1000 rpm.

The hydraulic ram pressure was read with a Sensotec model THE/4256-03 pressure transducer. The pressure transducer provides a 5.0-volt output signal over a 10,000-psig range. A Sola model SDP124-100 power supply provided 28 volts DC excitation to the pressure transducer. The piston displacement was read with two Schaevitz LVDTs, one attached to the ram (model DC-EC-1000) and the other to the frame (model DC-EC-250). A ±15 volt DC excitation voltage was supplied to the LVDTs by a Schaevitz PSD-4-15-001 power supply. The LVDTs produce a linear ±10V DC output signal over a range of 50 mm and 12.7 mm, respectively. The input and output voltages were read by an Agilent model 34970A digital multimeter and an Agilent 34901A 20-channel multiplexer. For the Expancel tests, the data were transferred via GPIB to a PCI card in an Apple G4 running OS9. For the foam tests, data were transferred via Ethernet with a GPIB-ENET/100 controller to the same Apple G4, upgraded to OSX. It was found to be necessary to disconnect the computer from the external network while acquiring data. Otherwise, outside activity on the network would cause the data acquisition program to hang.

The data acquisition program was written with National Instruments LabVIEW 7.0 software. The program reads and displays the input and output voltages at a sampling rate of 1 Hz and writes the data as an ascii text file on the computer hard drive. Data are recorded over both the loading and unloading portions of the pressure cycle. The data acquisition program also converts the LVDT output voltages to inches of displacement and converts the pressure transducer voltages to ram pressure in psig. The reduction in surface area from the ram to the piston is used to calculate internal pressure in the die in kilobars. The small radial expansion of the die with pressure is neglected by the data acquisition program.

The Enerpac ram has a limited stroke of about 19 mm. This range is adequate for most specimens, but it was not possible to load the foam specimens to 3 GPa in one run

without exceeding the range. Consequently, it was necessary to back the piston out of the die, leaving the specimen in place, and insert a 12.7 mm long tungsten carbide spacer into the die in order to reach full pressure. The data sets for the three successful foam specimen tests thus consist of two pressure-displacement curves offset by 12.7 mm. In processing the data, it was necessary to piece the two pressure-displacement curves together to make a single curve. This was made easier because, in each instance, the initial pressure-displacement curve contains a portion of the stiffening part of the compression test.

Three Expancel specimens and five foam specimens were prepared. However, the first Expancel specimen tested, Expancel #3, was only compressed to a few hundred bars before the Enerpac ram ran out of stroke. The run was abandoned, and the data are not analyzed here. The first test on a foam specimen, Foam B1, was terminated below 0.7 GPa when the Enerpac ram again ran out of stroke. The specimen was pushed out of the die and left on a table. A few hours later it was observed that the compacted foam was expanding and had pushed the lid off of the specimen. The limited loading data for Foam B1 were analyzed and are included in this report. A compression test on a later foam specimen, Foam C3, failed because one of the sealing rings was slightly undersized. Tin was extruded past the sealing ring during loading, and the run was abandoned.

2.4 Data Reduction

2.4.1 Die Bore Expansion

Pressure is measured in the hydraulic ram and calculated for the die as the ratio of the cross-sectional area of the ram to the die bore. Since the die bore expands diametrically with the rise in internal pressure, the calculated pressures will be slightly higher than the true pressures if no correction is made. We multiplied our calculated pressures by 0.9851 to correct for die bore expansion, based on tabulated correction terms given in Stephens and Lilley (1967).

2.4.2 Friction Corrections

Frictional effects result in hysteresis in the pressure-displacement curves obtained with the solid medium press. Pressure is measured in the hydraulic ram that drives the piston into the die. Frictional forces resist the piston's motion, resulting in measured pressures that are higher than the sample pressure during loading and lower than the sample pressure during unloading. The uncorrected pressure displacement data therefore show a hysteresis loop with each pressure cycle (Figure 7).

The friction correction technique, due to Bridgman (1964a), assumes that friction is the same in magnitude, but opposite in sign, for the loading and unloading portions of the pressure cycle, so that the mean pressure at each displacement is the true pressure. Our data are measured at a fixed sampling rate, so that the recorded displacements usually do not match precisely on both portions of the pressure cycle. Therefore, a series of interpolation displacements was chosen, and the pressure data were interpolated to

correspond to the displacements. The loading and unloading pressures were then averaged at common displacements.

A backlash effect occurs as unloading begins that, if ignored, would cause the calculated friction corrections to diminish at high pressure, which is unrealistic (Bridgman, 1964a). Bridgman (1964b) removed the backlash artifact by graphically extending the unloading curve, and then calculating mean pressure from the extended portion of the unloading curve at high pressures. The extrapolation attempts to make the unloading curve lie parallel to the loading curve in the backlash region, with the result that the friction correction is constant, or nearly so, at high pressure. Grens (1970) adopted a simpler method, which we followed; he took the friction correction to be constant at its maximum value in the backlash region. Friction corrections for Expancel and epoxy foam specimens are shown in Figures 8 and 9, respectively. The friction corrections differ for every specimen, but seldom exceed 0.25 GPa.

Separate friction corrections were made for the nickel reference standard and for each specimen. Nickel Standard #1 (Carlson et al., 2005) was chosen as the reference standard. The nickel standard was compressed to 3 GPa in two separate tests. Data from the second test were used for calculating the nickel standard friction corrections as the pressure-displacement curves from that test very nearly close at zero pressure. The foam and crushed powder specimens were only compressed once, so that friction corrections had to be calculated from the first pressurization cycle.

2.4.3 Volume Calculations

The data reduction procedure for the solid medium compression tests derives from earlier work at LLNL by Stephens and Lilley (1967) and Weed (1984). The method is to compare the specimen volume to the volume of a gold or nickel reference standard at every pressure. Both metals have well-known pressure-volume relations. The use of a reference standard eliminates corrections for the contraction of the piston, anvil and backing plates and for stretching of the press frame (Stephens and Lilley, 1967).

The data reduction procedure is described with reference to Table 4, which contains data and calculated values for a portion of the loading curve for Foam B4. The pressure data are corrected for friction and die bore expansion before being entered into the table. The first column is a list of interpolation pressures. The second column contains displacements measured for a nickel standard, and the third column contains specimen displacements. The displacements in both columns have been interpolated to correspond to the pressures in column 1. The fourth column is the specimen displacement minus the nickel standard displacement at each pressure. The fifth column is used to remove the small net displacement at zero pressure. Relative volume changes (column 6) are calculated from the zeroed net displacements of column 5. The seventh column contains nickel standard volumes calculated from nickel $P\text{-}\Delta V/V_0$ data of Vaidya and Kennedy (1970). The powder specimen volumes (column 8) are found by subtracting the relative volume changes (column 6) from the nickel standard volumes (column 7). Specific volumes, found by dividing specimen volumes (column 8) by mass, are given in column

9. Column 10 contains specimen volumes at each pressure normalized by the initial volume.

2.4.4 Energy Calculations

The energy expended in compression to 3 GPa was found by numerically integrating the loading portion of the pressure-specific volume curve for each material. The numerical integration was performed with the "Integrate-Area" macro routine included in the *Kaleidagraph* software package. The area under the loading curve includes stored elastic strain energy, energy absorbed by the material and energy dissipated as heat. The recoverable stored energy was found by integrating the unloading portion of the pressure-specific volume curves. No attempt was made to determine heat loss from the specimens.

2.4.5 Kawakita Model

Several empirical relationships between hydrostatic pressure and powder volume have been proposed. Equation (1), due to Kawakita and Ludde (1970), was found to provide an excellent fit between relative volume compaction, C, and pressure, P, for several granular materials (Carlson et al., 2005).

$$C = (V_0\text{-}V)/V_0 = (abP)/(1+bP) \quad (1)$$

where V_0 is the initial powder volume, V is volume at pressure, and a is the initial (zero pressure) porosity. Parameters a and b can be estimated by linear regression after rearranging equation (1) as

$$P/C = (1/a)\ P + 1/ab. \quad (2)$$

The P/C parameter can be interpreted as the secant bulk modulus of the material (Hayward, 1974). The initial porosity is found from the regression slope and the intercept gives an estimate of the room pressure bulk modulus (Hayward, 1974).

3. Results

3.1 Expancel 550 DU 40

The Expancel specimens experienced a great deal of permanent deformation below 0.1 GPa on the first pressure cycle, in which both specimens shortened by about 1.3 cm (Figure 10). A further shortening of about 0.4 cm occurred between 0.1 and 3 GPa, and was almost entirely recovered on unloading. The pressure-displacement curves for the two Expancel specimens agree very well, but the initial lengths of two specimens differed slightly because of problems filling the canisters. Expancel #1, which was initially about 0.3 mm shorter than Expancel #2, experienced somewhat more deformation.

Pressure-volume curves (Figure 11) reveal that a permanent reduction in volume of more than 60% occurred below 0.1 GPa for both Expancel specimens. The permanent volume

reduction at low pressure is attributed to the removal of porosity. The pycnometer measurements indicated 44-45% porosity for the Expancel specimens, but this may only include the porosity between the microspheres. The total porosity could be considerably higher if the microspheres are impermeable to helium. The large permanent volume reduction below 0.1 GPa suggests that the initial porosity was at least 60%. The slopes of the P-V curves gradually steepen between 0.1 GPa and 1 GPa. The stiffening may also be due to porosity removal. If so, the initial porosity would have been more than 70% because the P-V curves only become linear below a relative volume of 0.3.

Pressure is plotted against specific volume for both Expancel specimens in Figure 12. An apparent grain density of 1.137 g/cm^3 was found from pycnometer measurements. Both specimens compact to a density of over 1.67 g/cm^3 under 0.1 GPa pressure. The value of 1.67 g/cm^3 provides a lower bound for the grain density. The density of the shell material is likely to be greater than 1.67 g/cm^3 because some porosity may remain at 0.1 GPa and because the microspheres contain isopentane, which has a density of 0.60 g/cm^3 at room pressure.

3.2 Epoxy Foam

Foam B1 was compressed to about 0.62 GPa in a single pressure cycle and was then removed from the die. A few hours later, the compressed foam had expanded sufficiently to push the lid partially off the canister. The compressed foam appears to be a soft, gelatinous mass containing small pockets of trapped gas. Expansion of the trapped, pressurized gas, combined with a viscoelastic response of the foam polymer, presumably accounts for the expansion. The specimen was photographed under an optical microscope (Figure 13).

Pressure versus displacement curves for the epoxy foam and crushed foam powder are shown in Figure 14. The crushed foam specimen had a much lower initial porosity (45%) than the intact foam specimens (79-82%) and underwent much less deformation at low pressures. The foam specimens shortened by 1.6 to 1.8 cm, whereas the powder specimen shortened by only 1.0 cm below 0.1 GPa. The foam shortened more, and the powder less, than the Expancel specimens.

Pressure-volume curves for epoxy foam and crushed foam powder are shown to 3 GPa in Figure 15, and to 0.1 GPa in Figure 16. The foam specimens underwent permanent volume reductions of 77-85% below 0.05 GPa, and the crushed foam powder underwent a volume reduction of about 45%. The pressure-volume curves stiffen dramatically near 0.02 GPa. The measured volume reductions are in good, general agreement with the initial porosities. The specimens having the highest initial porosities, B1 and B5, show the largest volume reductions, and Foam C3, which had the smallest initial porosity, shows the least volume reduction. However, the volume reductions of 77-85% at 0.05 GPa are somewhat broader than the initial foam porosities of 79-82%. The relatively small volume reductions above 0.1 GPa likely represent deformation of the foam polymer and are recovered on unloading.

Ceramic microspheres studied by Carlson et al. (2005) are a lightweight, high-porosity material. At 85%, their porosity is comparable to the epoxy foam. Their structure is similar to the Expancel microspheres, except that their outer shells are much more brittle. A pressure-volume curve for ceramic microspheres from Carlson et al. (2005) is shown along with the materials from this study in Figure 17. All of the materials undergo large volume reductions at low pressure, but the ceramic microspheres recover very little deformation on unloading and retain significant porosity at high pressures in contrast to the materials in this study. The pressure-volume curves for the foam and Expancel specimens resemble those obtained by Stephens and Lilley (1966) for partially-saturated alluvium. The alluvium pressure-volume curves also show much volume recovery on unloading.

Pressure versus specific volume for "mean" foam and crushed foam powder is shown in Figure 18. The "mean" foam was obtained by averaging the specific volumes of foam specimens B4, B5 and C3 at every pressure. Foam B1 was not included. Although the initial specific volumes differ greatly, the curves are well matched after most of the initial porosity has been destroyed. At high pressure, the foam appears to be stiffer than the crushed foam powder, but this may be an experimental artifact. The foam compression tests incorporate an additional tungsten carbide spacer at high pressures and the jacket walls have become quite thick due to the extensive shortening. Figure 19 shows a portion of the same data as Figure 18. The grain density obtained from the pycnometer measurements is indicated in the figure. The foam stiffens dramatically near the full grain density on loading and remains near full density on unloading. However, the agreement is not perfect: the foam specimens appear to have undergone a bit more volume reduction at low pressure than might be expected from the grain density. It was noted in Carlson et al. (2005) that powder grain densities calculated from our pycnometer measurements tend to be slightly lower than the values quoted by the manufacturers. If our grain density were to increase by 5% from 1.14 to 1.2 g/cm^3, corresponding to a specific volume of 8.33 cm^3/g, the agreement would be much improved, as the P-V curves appear fairly linear below 8.33 cm^3/g. Alternately, the displacements measured in the compression tests may be slightly too large. A bit of dead air space in the piston/specimen/anvil assembly might cause the measured displacements to be overly large.

3.3 Energy and Compressibility

The energy expended in compressing these materials to 3 GPa was found by integrating the loading portions of their respective pressure-volume curves. Relatively little energy is required to compact these materials, as most of the porosity reduction occurs at pressures below 0.1 GPa. Moreover, the energy expended above 0.1 GPa is mostly recovered on unloading. The raw loading and unloading curves lie nearly parallel to each other above 0.1 GPa for both the epoxy foam and the Expancel microspheres (e.g. Figure 7) in contrast to most of the granular materials studied by Carlson et al. (2005). After the pressures are corrected for friction, the curves overlap above 0.1 GPa. Consequently, the areas under the loading and unloading curves are nearly the same for each specimen (Figure 20). The net energy, which includes the energy absorbed by these materials, is small.

Compressibility, calculated as the slope of the pressure-volume curve, falls by three orders of magnitude with pressure for the two Expancel specimens (Figure 21). The compressibility results agree very well for the two Expancel specimens. Bulk modulus is the inverse of compressibility. The Expancel bulk modulus increases rapidly below 0.1 GPa, then linearly over a wide range of pressure (Figure 22). The data are erratic at high pressure because the incremental volume changes are small. At 3 GPa the Expancel bulk modulus is about 23 or 24 GPa.

The Expancel microspheres contain a small quantity of liquid isopentane. At pressures between 0.1 and 0.65 GPa, the Expancel bulk modulus closely matches that of isopentane (Figure 23). The isopentane data are from Bridgman (1964c). If the Expancel shells have little rigidity, the applied pressure should collapse the microsphere shells onto the liquid isopentane. The isopentane inclusions may then control the material stiffness.

The compressibility of crushed foam powder (Figure 24) is generally comparable to that of Expancel, but the crushed foam powder is somewhat less compressible at high pressures. The bulk modulus of the crushed foam increases linearly over a broad range of pressure between 0.5 and 2.0 GPa (Figure 25). At 3 GPa the crushed foam bulk modulus is about 40 GPa.

3.4 Kawakita Model Fits

Porosities were estimated by fitting pressure-volume data to the Kawakita model (Table 5). Both methods yield initial porosities of about 80% for the foam, but the foam porosities derived from the Kawakita model are mostly higher (Figure 26). The pycnometer data yield porosities of about 45% for the Expancel microspheres, but the Kawakita model fits yield initial porosities of about 75%. If the outer shells of the Expancel microspheres are impermeable to helium, then the pycnometer data would fail to capture the porosity inside the microspheres. If so, the pycnometer data provide an estimate of the "exterior" porosity, i.e. – the void space between the microspheres (45%), and the Kawakita model provides and estimate of the total porosity (75%). The latter value is much closer to the 85% porosity found for the hollow ceramic microspheres (Carlson et al., 2005).

The Kawakita model fits to the two Expancel specimens are shown in Figures 27-28. Only 5% of the data are plotted for clarity. The Expancel bulk modulus at zero pressure, taken from the regression intercepts, is about 0.05 to 0.06 GPa. The regression slopes, 1.3106 for Expancel #1 and 1.3414 for Expancel #2, correspond to initial porosities of 76% and 75%, respectively. Since the pycnometer measurements indicate an "exterior" porosity of 44-45%, the other 30% presumably represents the void space inside the hollow microspheres. At 75% porosity and bulk density of 0.63 g/cm^3, the Expancel grain density is about 2.5 g/cm^3. If Expancel #3 is assumed to have a grain density of 2.5 g/cm^3, then its initial porosity would be 74.5%, similar to the other Expancel specimens.

The Kawakita model fit to the crushed foam powder is shown in Figure 29. Again, only

5% of the data are plotted for clarity. The bulk modulus at room pressure is 0.09 GPa. The regression slope of 1.764 corresponds to an initial porosity of 57%, which is clearly higher than the 45% porosity found from the pycnometer data. At 57% porosity, the foam grain density would be 1.50 g/cm^3. The Kawakita model regression fits to the foam data are shown in Figures 30-33. The regression slopes for Foam B1, B4 and B5 predict initial porosities between 84% and 87%, higher than the 80% porosity found from the pycnometer measurements. The regression slope for Foam C3 yields an initial porosity of 79% in excellent agreement with the pycnometer data. Estimates for the foam bulk modulus at room pressure range from 0.002 to 0.01 GPa.

4. Summary and Conclusions

Pressure-volume measurements were made at ambient temperature to 3 GPa in a solid medium press on dry, unexpanded Expancel microspheres, epoxy foam and one specimen of crushed foam powder. These soft, porous materials undergo dramatic reductions in volume at low pressure, and then stiffen abruptly at or near full densification. Most of the volume reduction is permanent, but some volume recovery is evident on unloading. The energy expended in compaction was estimated by numerically integrating the pressure-specific volume curve for each material. Relatively little energy is expended in compacting these materials because most of the volume reduction occurs at low pressure. Compressibility and bulk modulus were calculated from the slopes of the P-V curves for the Expancel microspheres and the crushed foam powder. The Expancel bulk modulus was found to match closely that of isopentane at pressures above 0.1 GPa. Each of the Expancel microspheres contains a small quantity of isopentane, which apparently controls the material's deformation after the porosity has been removed. The initial porosity of 45% obtained for the Expancel microsphere specimens from the helium pycnometer measurements was found to be far too low. The microsphere shells are apparently impermeable to helium, and the interior void space was missed. The Kawakita model provided an initial porosity of 75% for the Expancel specimens, which is in much better agreement with the pressure-volume data.

Acknowledgements

Carl Boro, William Ralph and David Ruddle provided technical assistance. William Ralph and Chantel Aracne provided photographs of the foam.

References

Akzo Nobel, 2004. "Expancel and Elasticity," Technical Bulletin No. 1, Akzo Nobel Corp., 5 p.

Bridgman, P. W., 1964a. "Linear compressions to 30,000 kg/cm^2 including relatively incompressible substances," in Collected Experimental Papers, vol. VI, Harvard University Press, Cambridge, MA, Paper No. 168, 3933-3978.

Bridgman, P. W., 1964b. "The compression of 46 substances to 50,000 kg/cm^2," in Collected Experimental Papers, vol. VI, Harvard University Press, Cambridge, MA, Paper No. 134, pp. 3411-3441.

Bridgman, P. W., 1964c. "The volume of eighteen liquids as a function of pressure and temperature," in Collected Experimental Papers, vol. IV, Harvard University Press, Cambridge, MA, Paper No. 89, 2431-2479.

Carlson, S. R., B. P. Bonner, F. J. Ryerson and M. M. Hart, 2005. "Compaction of ceramic microspheres, spherical molybdenum powder and other materials to 3 GPa," Internal Report. Lawrence Livermore National Laboratory, Livermore, CA.

Gibson, L. J. and M. F. Ashby, 1982. "The mechanics of three-dimensional cellular materials," *Proc. R. Soc. Lond.*, A **382**, 43-59.

Grens, J. Z., 1970. "Computer operation of a compressibility testing apparatus," Lawrence Radiation Laboratory, Livermore, CA, UCIR-457, 14 p.

Hayward, A. T. J., 1971. "How to measure the isothermal compressibility of liquids accurately, " *J. Phys. D: Appl. Phys.*, **4**, 938-950.

Heard, H. C. and D. R. Stephens, 1970. "Compressibility and strength behavior of Diagonal Line alluvium," Lawrence Radiation Laboratory, Livermore, CA, UCID-15736, 8 p.

Kawakita, K. and K. H. Ludde, 1970. "Some considerations on powder compression equations," *Powder Technology*, **4**, 61-68.

Stephens, D. R. and E. M. Lilley, 1966. "Static PV curves of cracked and consolidated earth materials to 40 kilobars," Lawrence Radiation Laboratory, Livermore, CA, UCRL-14711, 43 p.

Stephens, D. R. and E. M. Lilley, 1967. "Procedure for pressure-volume runs on rocks," Lawrence Radiation Laboratory, Livermore, CA, UCID-15070, 12 p.

Vaidya, S. N. and G. C. Kennedy, 1970. "Compressibility of 18 metals to 45 kbar," *J. Phys. Chem. Solids,* **31**, 2329-2345.

Weed, H. C., 1984. "Pressure-density behavior for AlN, Al_2O_3, SiO_2, TiB_2 and TiC powders up to 3.5 GPa," Lawrence Livermore National Laboratory, Livermore, CA, UCID-20302, 31 p.

Table 1. Chemical Components of the Foam

Supplier	Common Name	Product Name	Part #
CIBA-Gigy Corp.	Cycloaliphatic Epoxy Resin	Araldite CY 179	2140641
Union Carbide Chemicals & Plastics	Vinyl Cyclohexene Dioxide	Cycloaliphatic Epoxy Resin ERL-4206	2140642
U. S. Borax & Chemical Corp.	Tri-M, P-Cresyl Borate	Borester 8	2140643

Table 2. Powder Densities from Pycnometer Measurements

Specimen	Mass (g)	Volume (cm^3)	Density (g/cm^3)
Expancel 550 DU 40	1.588	1.397±0.005	1.137
Crushed Foam 1	1.811	1.586 ±0.011	1.142
Crushed Foam 2	1.815	1.592 ±0.017	1.140

Table 3. Specimen Statistics

Specimen	Mass (g)	Volume (cm^3)	Bulk Density (g/cm^3)	Grain Density[1] (g/cm^3)	Porosity[1] (%)
Expancel 1	1.6158	2.590	0.624	1.137	45.1
Expancel 2	1.6663	2.623	0.635	1.137	44.1
Expancel 3	1.7345	2.723	0.637	1.137	44.0
Foam B1	0.5477	2.723	0.201	1.141	82.3
Foam B4	0.6159	2.723	0.226	1.141	80.3
Foam B5	0.5797	2.723	0.213	1.141	81.5
Foam C3	0.6476	2.723	0.238	1.141	79.4
Powder P1	1.7223	2.723	0.632	1.141	44.6

[1] The grain density and porosity values are lower bounds for the Expancel specimens as the microspheres may not be permeable to helium.

Table 4. Data Reduction Table (truncated) for Foam B4

1	2	3	4	5	6	7	8	9	10
Pres. (GPa)	**Std. D (cm)**	**SpecD (cm)**	**Net D. (cm)**	**Zer. D. (cm)**	**ΔV (cm^3)**	**Std. V (cm^3)**	**Vol. (cm^3)**	**Spec. V (cm^3/g)**	**V/V_0**
0.0000	0.0000e+00	0.0000	0.00000	0.00000	0.00000	2.72340	2.72340	4.42182	1.00000
0.0005	7.0218e-05	0.0027	0.00259	0.00259	0.00328	2.72339	2.72011	4.41648	0.998792
0.0010	1.4044e-04	0.0030	0.00287	0.00287	0.00364	2.72339	2.71975	4.41589	0.998658
0.0015	2.1065e-04	0.0034	0.00316	0.00316	0.00400	2.72338	2.71938	4.41529	0.998524
0.0020	3.0778e-04	0.0037	0.00341	0.00341	0.00432	2.72337	2.71905	4.41476	0.998402
0.0025	4.4832e-04	0.0041	0.00362	0.00362	0.00459	2.72336	2.71877	4.41431	0.998300
0.0030	5.7462e-04	0.0044	0.00385	0.00385	0.00488	2.72336	2.71848	4.41383	0.998192
0.0035	6.9042e-04	0.0048	0.00409	0.00409	0.00518	2.72335	2.71817	4.41333	0.998079
0.0040	8.0553e-04	0.0055	0.00474	0.00474	0.00600	2.72334	2.71734	4.41199	0.997775
0.0045	9.1955e-04	0.2163	0.21535	0.21535	0.27281	2.72333	2.45053	3.97878	0.899805
0.0050	1.0326e-03	0.3420	0.34096	0.34096	0.43193	2.72333	2.29139	3.72040	0.841372
0.0055	1.1403e-03	0.4969	0.49577	0.49577	0.62804	2.72332	2.09528	3.40197	0.769360
0.0060	1.2479e-03	0.7120	0.71072	0.71072	0.90034	2.72331	1.82297	2.95985	0.669373
0.0065	1.3612e-03	0.8570	0.85568	0.85568	1.08397	2.72330	1.63933	2.66169	0.601943
0.0070	1.4758e-03	0.9573	0.95584	0.95584	1.21086	2.72330	1.51244	2.45565	0.555348
0.0075	1.6005e-03	1.0682	1.06655	1.06655	1.35111	2.72329	1.37218	2.22793	0.503848
0.0080	1.7325e-03	1.2392	1.23748	1.23748	1.56764	2.72328	1.15564	1.87635	0.424339
0.0085	1.8136e-03	1.3849	1.38307	1.38307	1.75207	2.72327	0.971208	1.57689	0.356616
0.0090	1.8681e-03	1.4397	1.43781	1.43781	1.82141	2.72327	0.901854	1.46429	0.331150
0.0095	1.9225e-03	1.4830	1.48109	1.48109	1.87625	2.72326	0.847013	1.37524	0.311013
0.0100	1.9770e-03	1.5349	1.53289	1.53289	1.94186	2.72325	0.781391	1.26870	0.286917
0.0105	2.0314e-03	1.5693	1.56728	1.56728	1.98544	2.72325	0.737809	1.19794	0.270915
0.0110	2.0962e-03	1.5894	1.58728	1.58728	2.01077	2.72324	0.712473	1.15680	0.261611
0.0115	2.1611e-03	1.6103	1.60810	1.60810	2.03714	2.72323	0.686096	1.11397	0.251926
0.0120	2.2260e-03	1.6258	1.62358	1.62358	2.05676	2.72322	0.666467	1.08210	0.244719
0.0125	2.2903e-03	1.6395	1.63722	1.63722	2.07403	2.72322	0.649189	1.05405	0.238374

Table 5. Grain Densities and Initial Porosities from the Kawakita Model

Specimen	**1/a**	**1/(ab) (GPa)**	**Bulk Density (g/cm^3)**	**Grain Density[1] (g/cm^3)**	**Porosity[2] (%)**
Expancel 1	1.3106	0.0537	0.624	2.63	76.3
Expancel 2	1.3414	0.0599	0.635	2.50	74.5
Foam B1	1.1520	0.00231	0.201	1.52	86.8
Foam B4	1.1956	0.0104	0.226	1.38	83.6
Foam B5	1.1462	0.00795	0.213	1.67	87.2
Foam C3	1.2615	0.0100	0.238	1.15	79.3
Powder P1	1.7640	0.0866	0.632	1.46	56.7

[1] Calculated as bulk density/(1 – void ratio).

[2] Calculated as 100/(1/a).

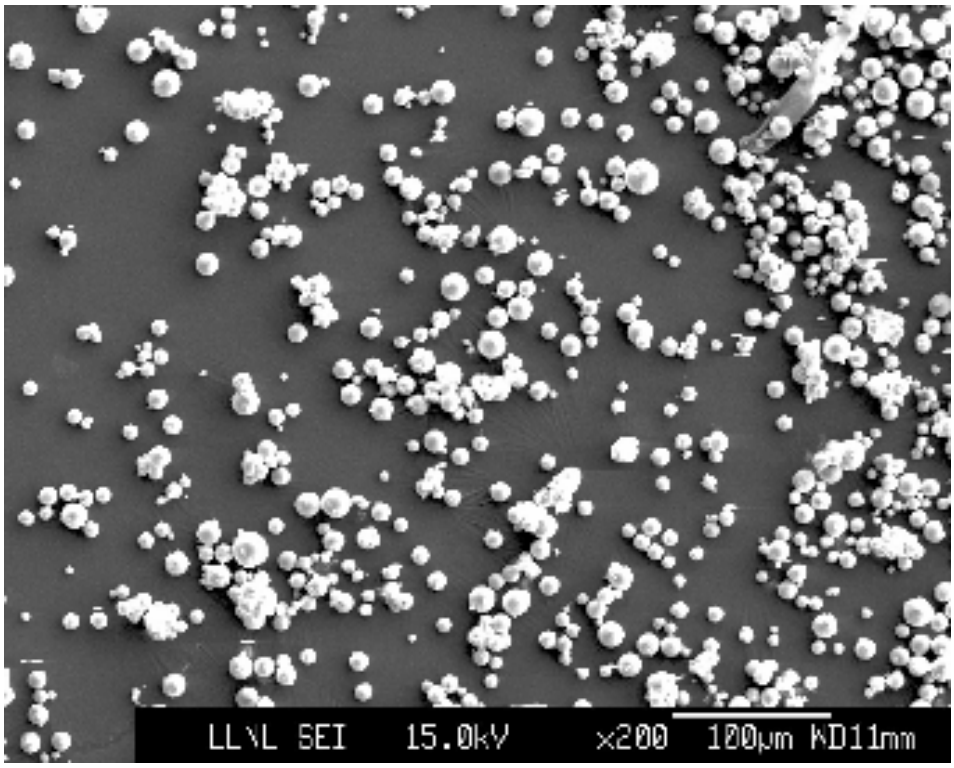

a.

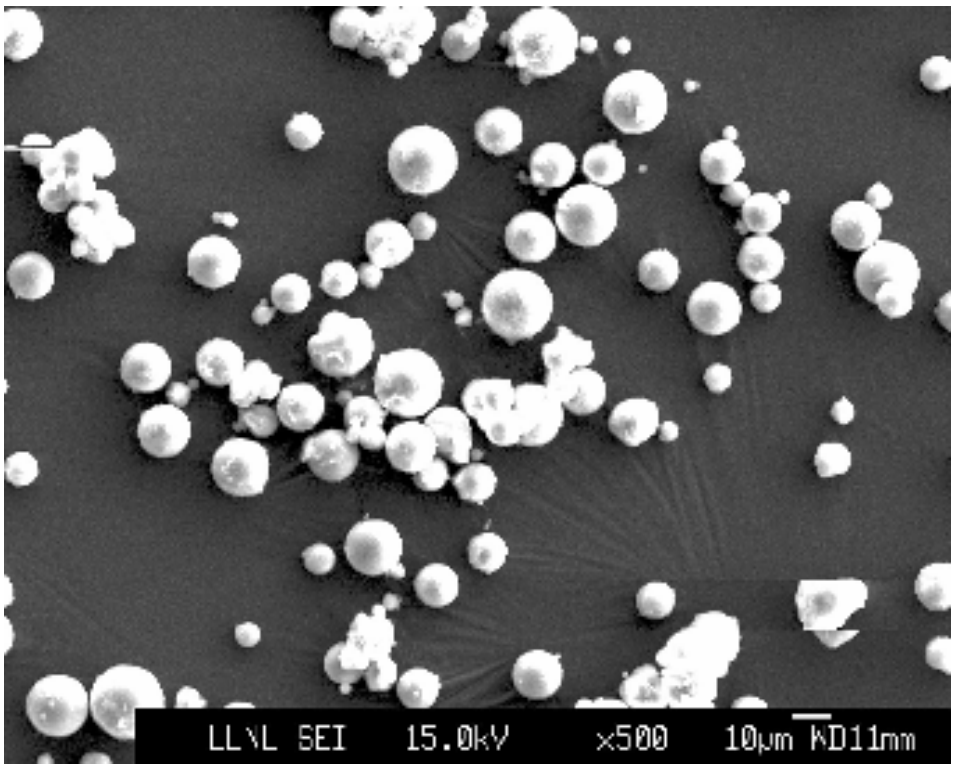

b.

Fig. 1. Expancel 551 DU 40 microspheres. Magnification: a.) 200x. b.) 500x.

Fig. 2. Stainless steel container, lower portion, and foam.

Fig. 3. Cross-section through the steel container and enclosed foam. A thin skin of dense material can be seen on the exterior of the foam. A few relatively large pores can be seen in the interior.

Fig. 4. Top portion of the foam. The thin, dense skin has largely broken off from the top of the foam.

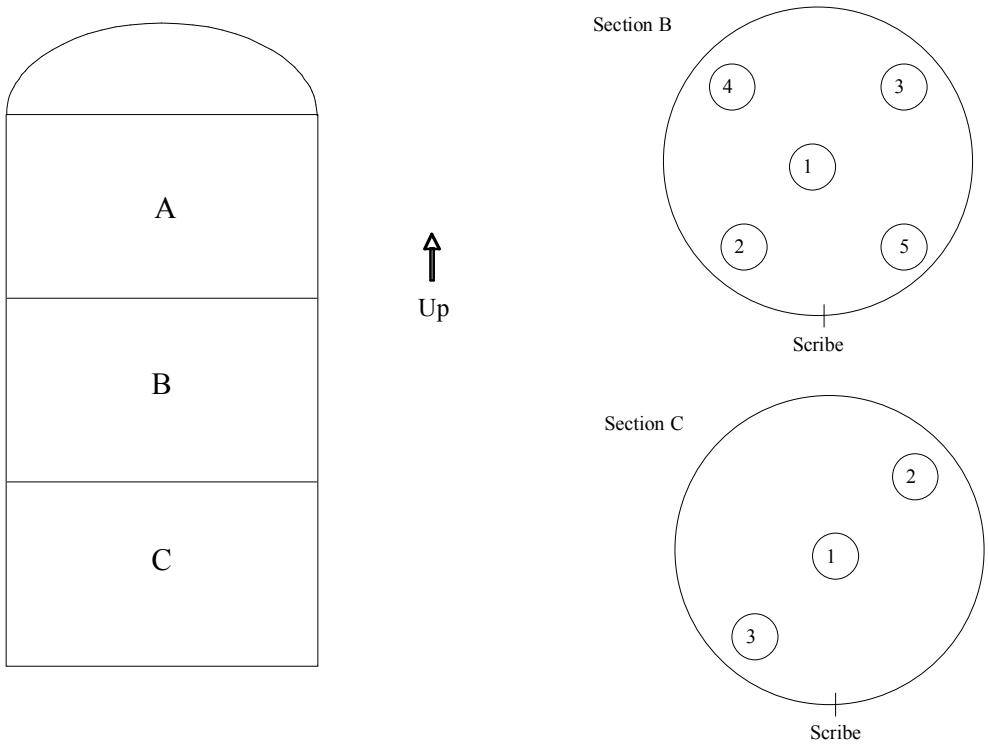

a. b.

Fig. 5. a.) Schematic diagram of foam cylinder and b.) approximate core locations in plan view. A scribe line was drawn to maintain relative alignment, and the foam was cut with a hand saw into three sections of approximately equal height, labeled A, B and C starting from the top. Small cores were cut with a cork borer and numbered as shown at right.

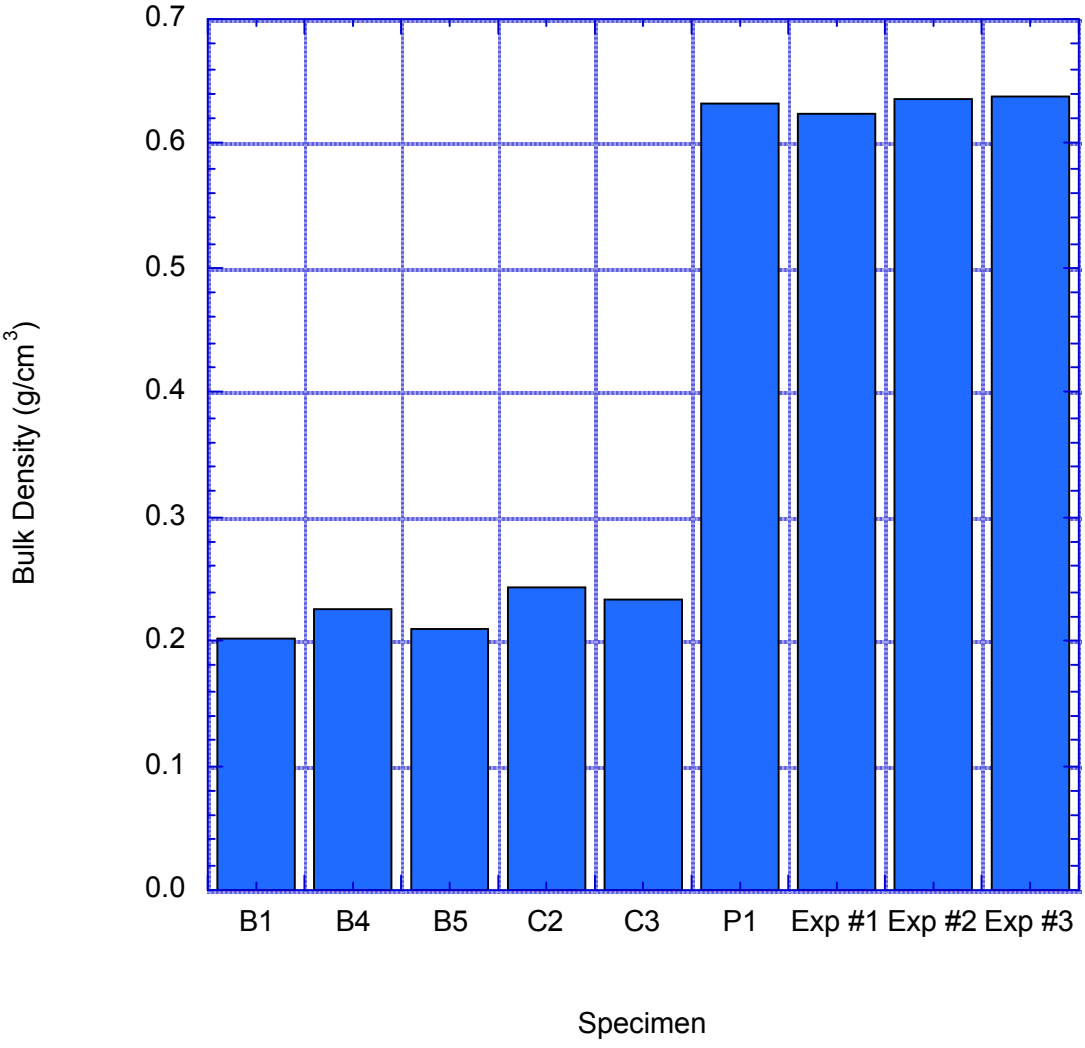

Fig. 6. Initial bulk density for epoxy foam (B1 – C3), crushed foam powder (P1) and Expancel specimens.

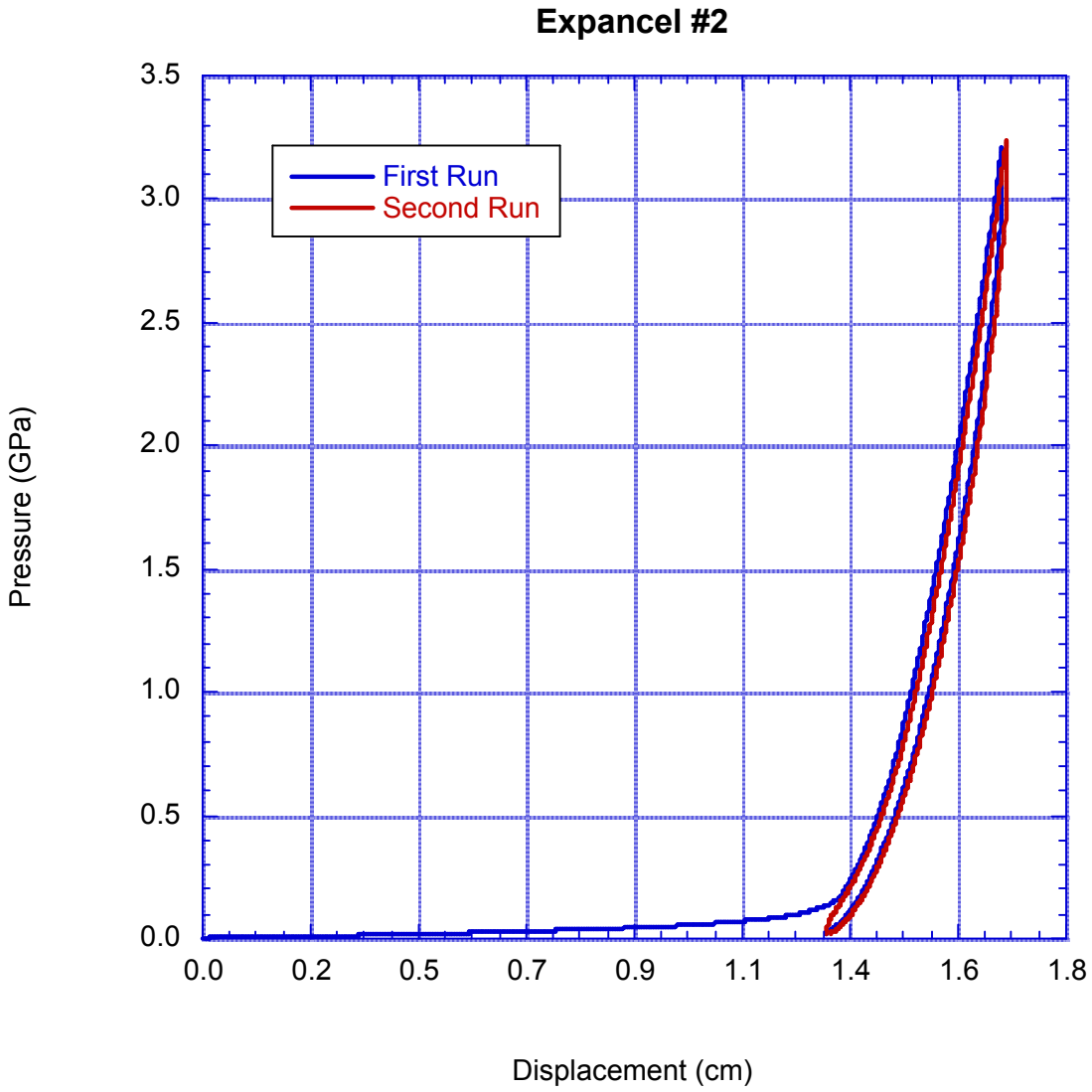

Fig. 7. Measured displacements for Expancel #2 over two pressure cycles to 3 GPa. The first cycle, in blue, results in much permanent deformation. The second pressure cycle largely repeats the high-pressure portion of the first cycle. The hysteresis loops, which occur for both cycles, are due to friction. The hysteresis loop for the second pressure cycle nearly closes at room pressure.

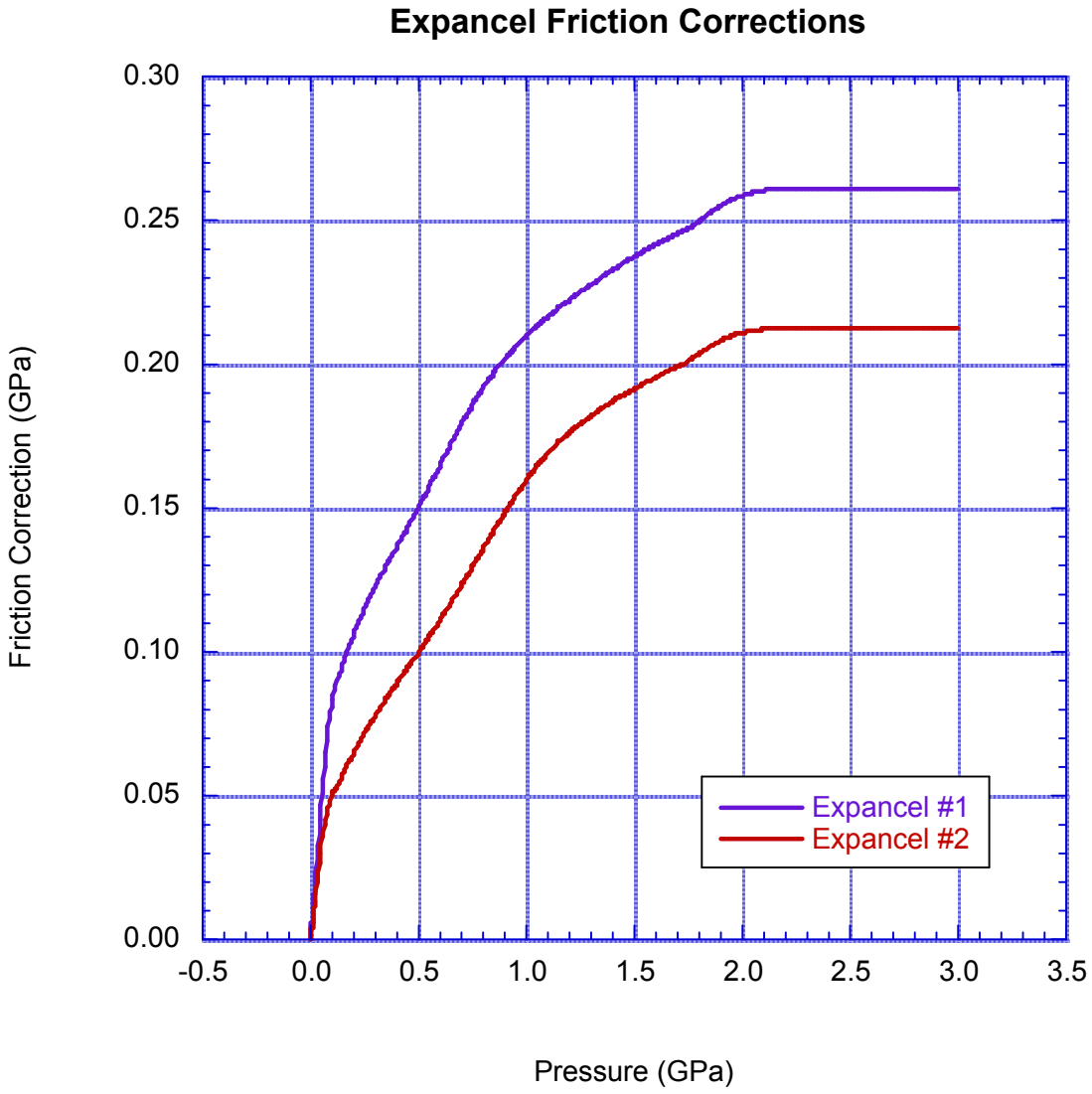

Fig. 8. Friction corrections for the Expancel specimens. Friction reaches a peak value at about 2 GPa and is assumed constant thereafter.

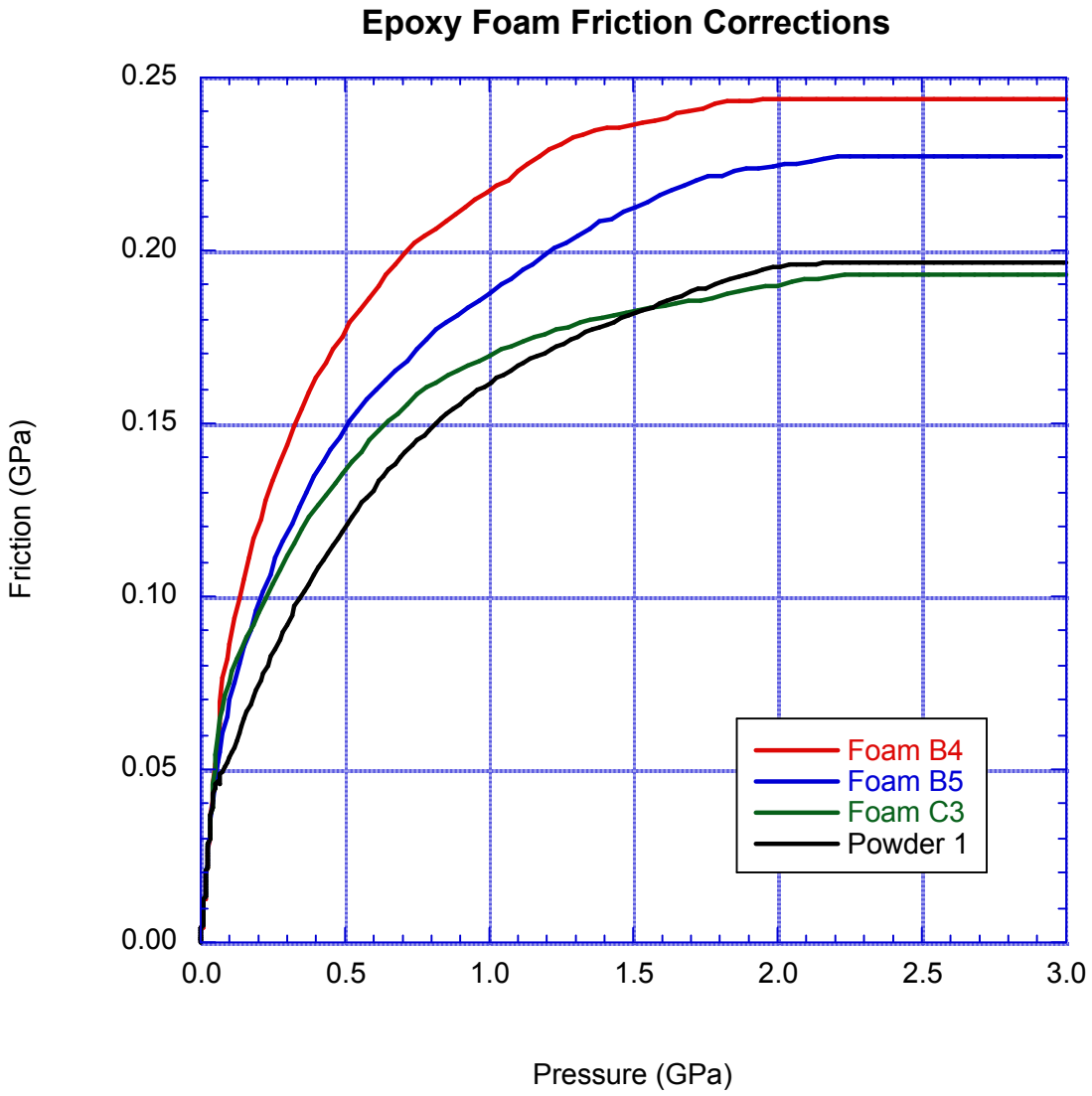

Fig. 9. Friction corrections for the foam specimens. Friction varies considerably from specimen to specimen.

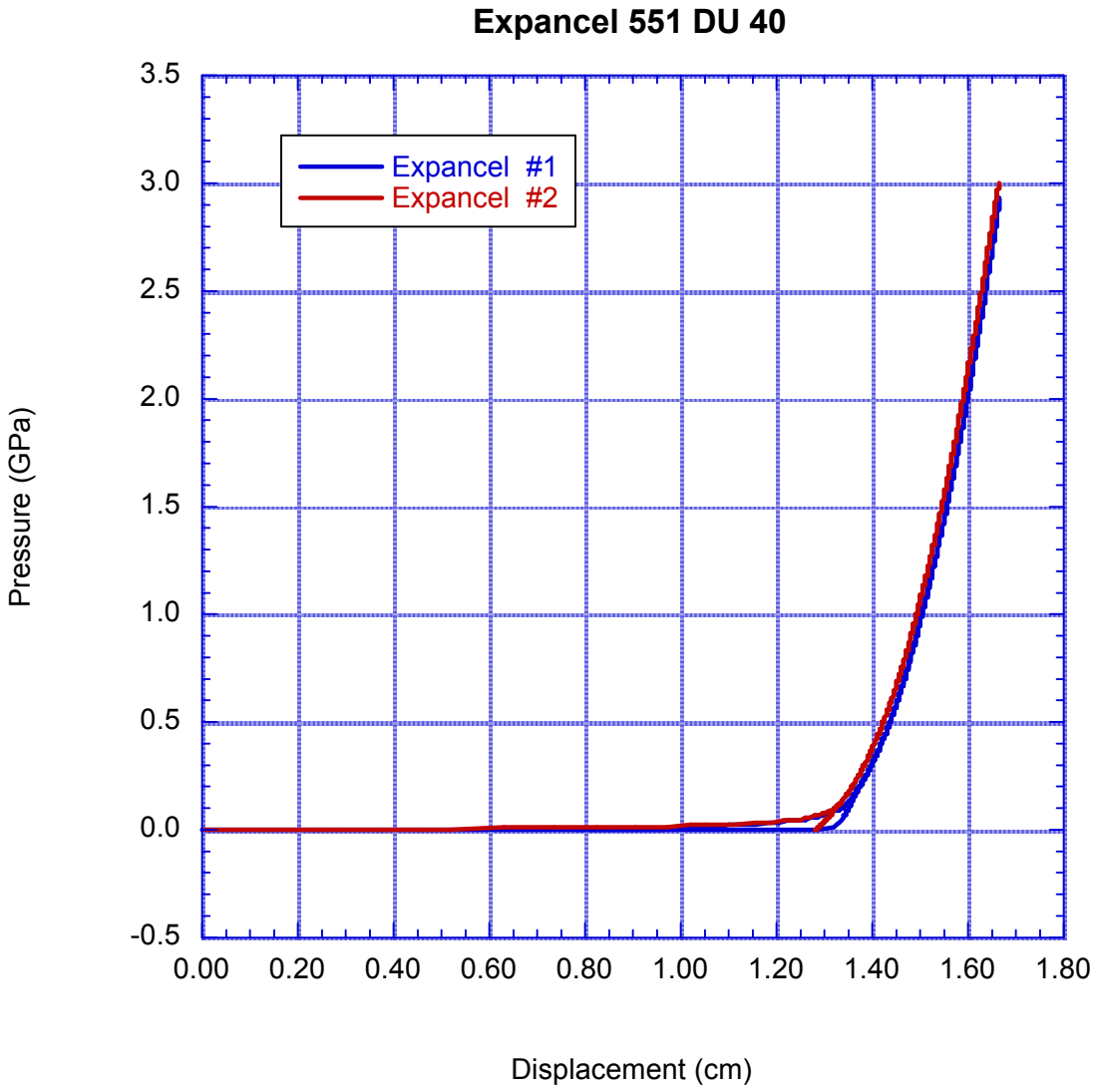

Fig. 10. Pressure vs. displacement curves for two Expancel specimens. The data are corrected for friction. Because of a problem filling the tin canisters, the initial lengths of two specimens differed slightly. Expancel #1, which was about 0.03 cm shorter than Expancel #2, has undergone somewhat more deformation.

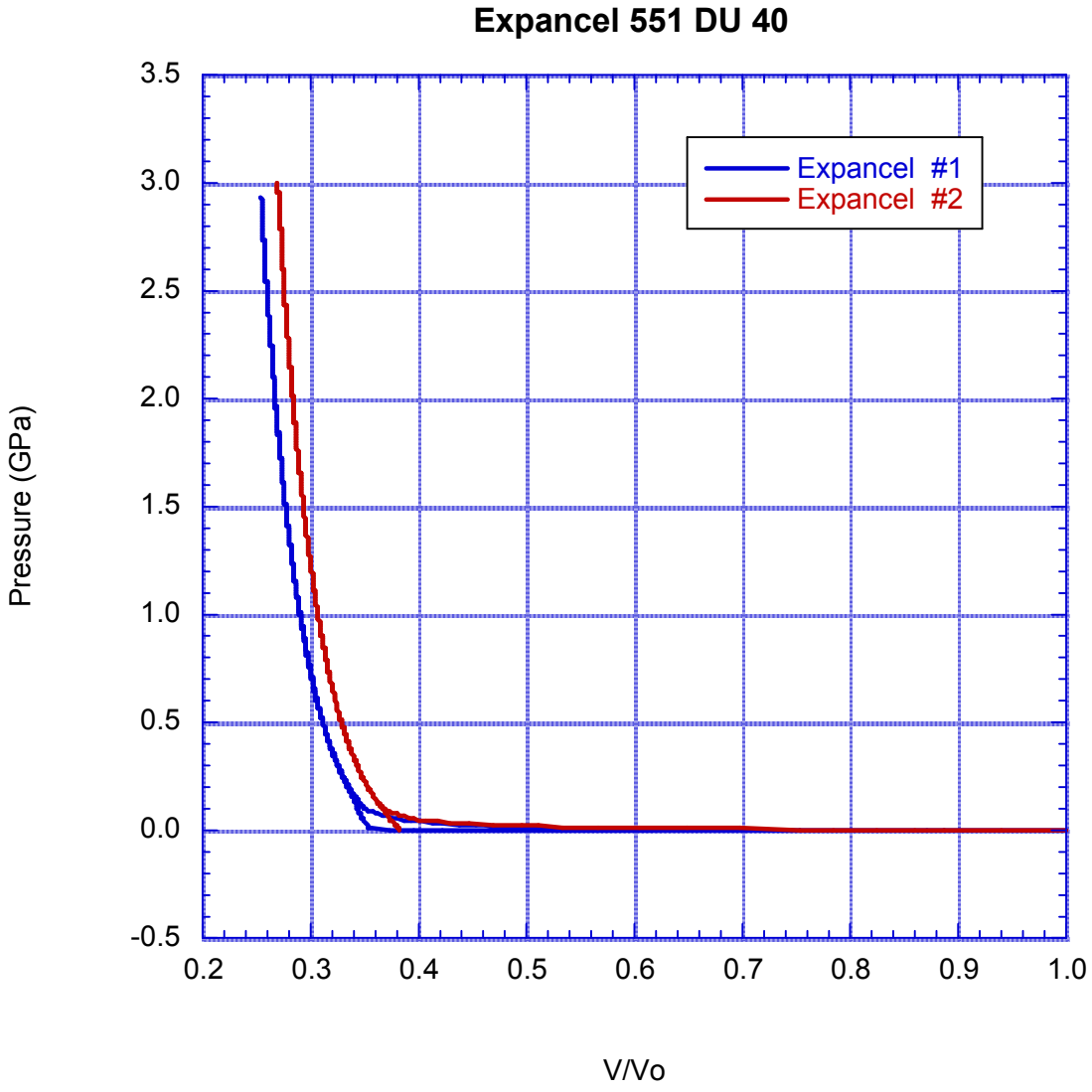

Fig. 11. Pressure-volume curves for dry, unexpanded Expancel. A permanent volume reduction of more than 60% occurred below 0.1 GPa for both specimens. The slopes of the P-V curves gradually steepen above 0.1 GPa as additional porosity is removed, but essentially all volume reduction above 0.1 GPa is recovered on unloading.

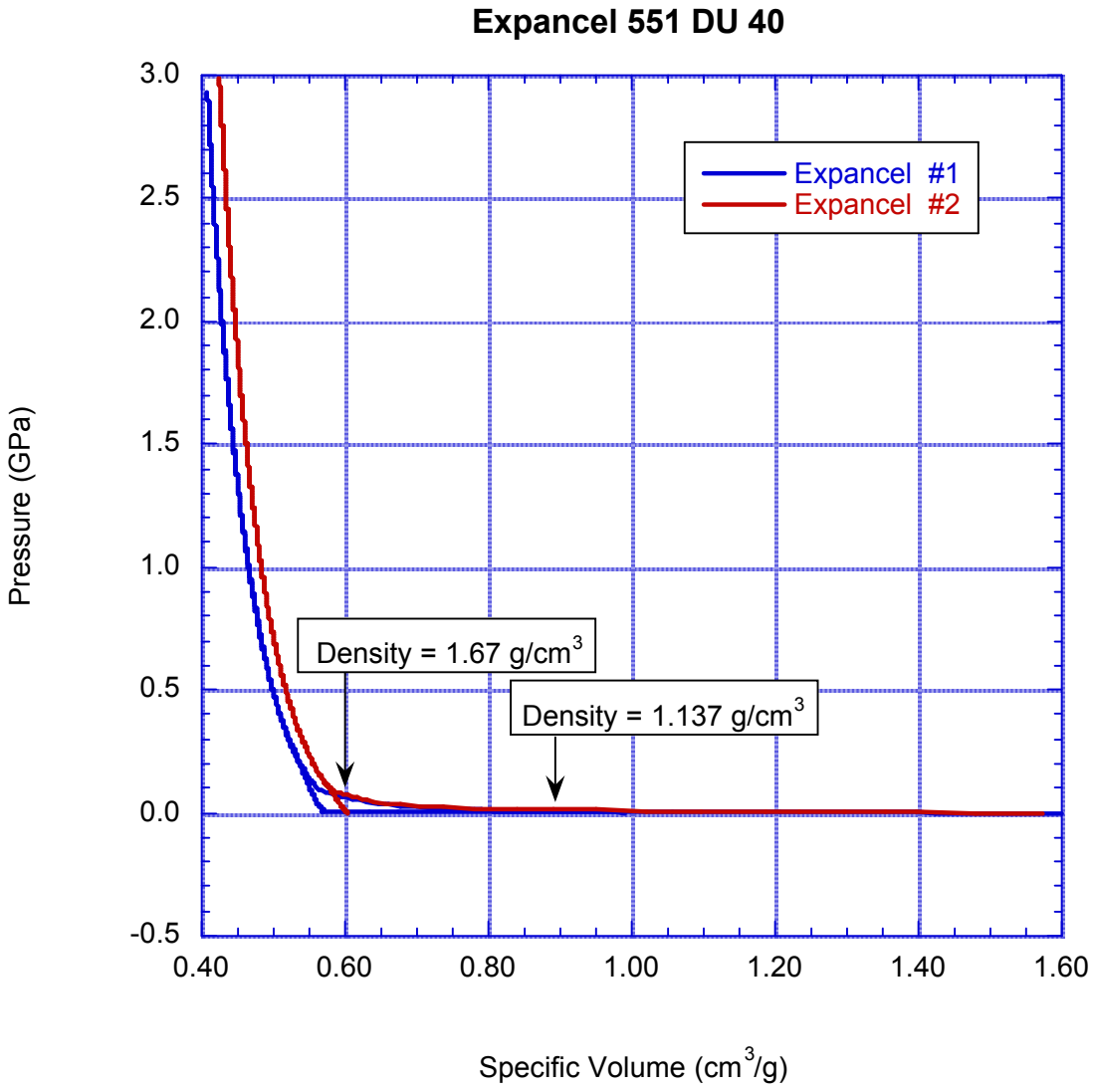

Fig. 12. Pressure vs. specific volume for Expancel specimens. A grain density of 1.137 g/cm^3 was found from the pycnometer measurements. However, both specimens compact to a density of about 1.67 g/cm^3 under a pressure of 0.1 GPa, suggesting that the helium pycnometer measurements missed much of the initial Expancel porosity.

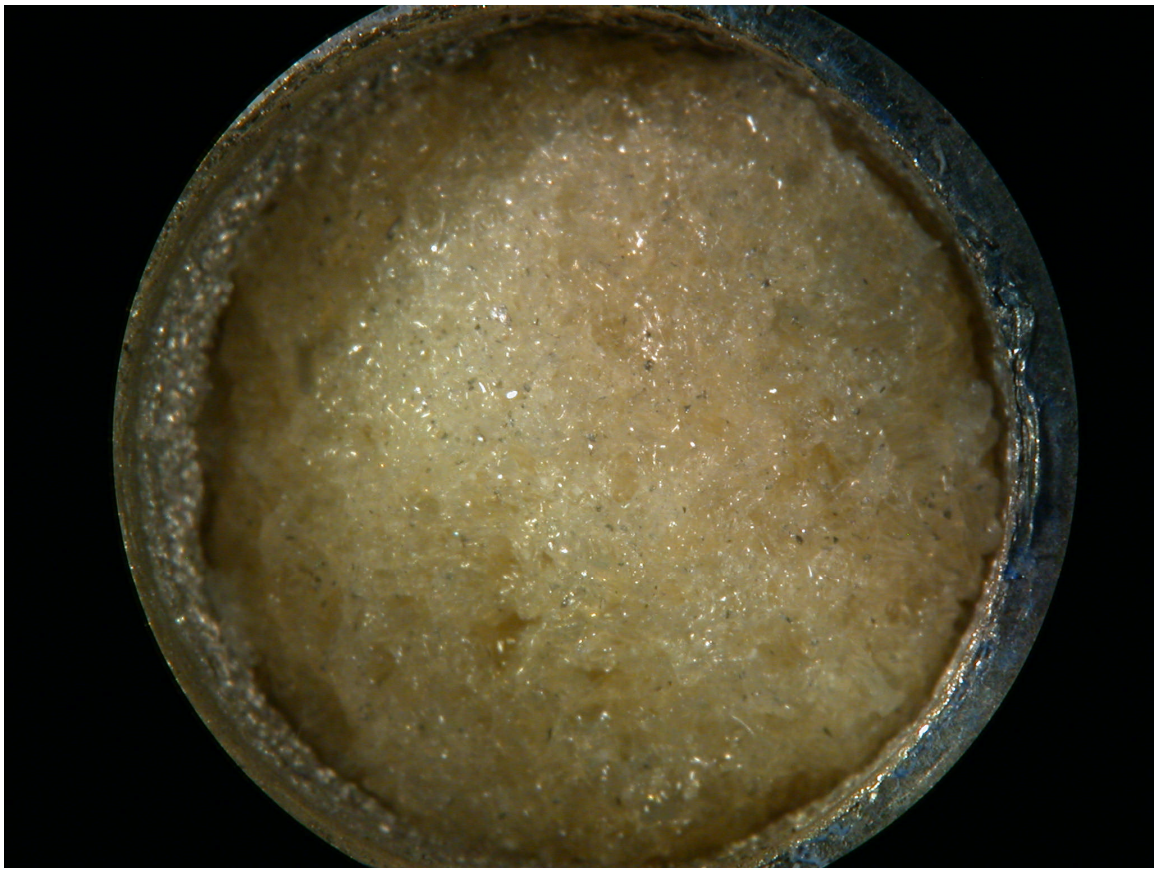

Fig. 13. Photograph of Foam B1 after a pressure cycle to 0.62 GPa. The compacted foam expanded on decompression, pushing the tin lid and indium disk free from the specimen jacket. The specimen width is 12.7 mm.

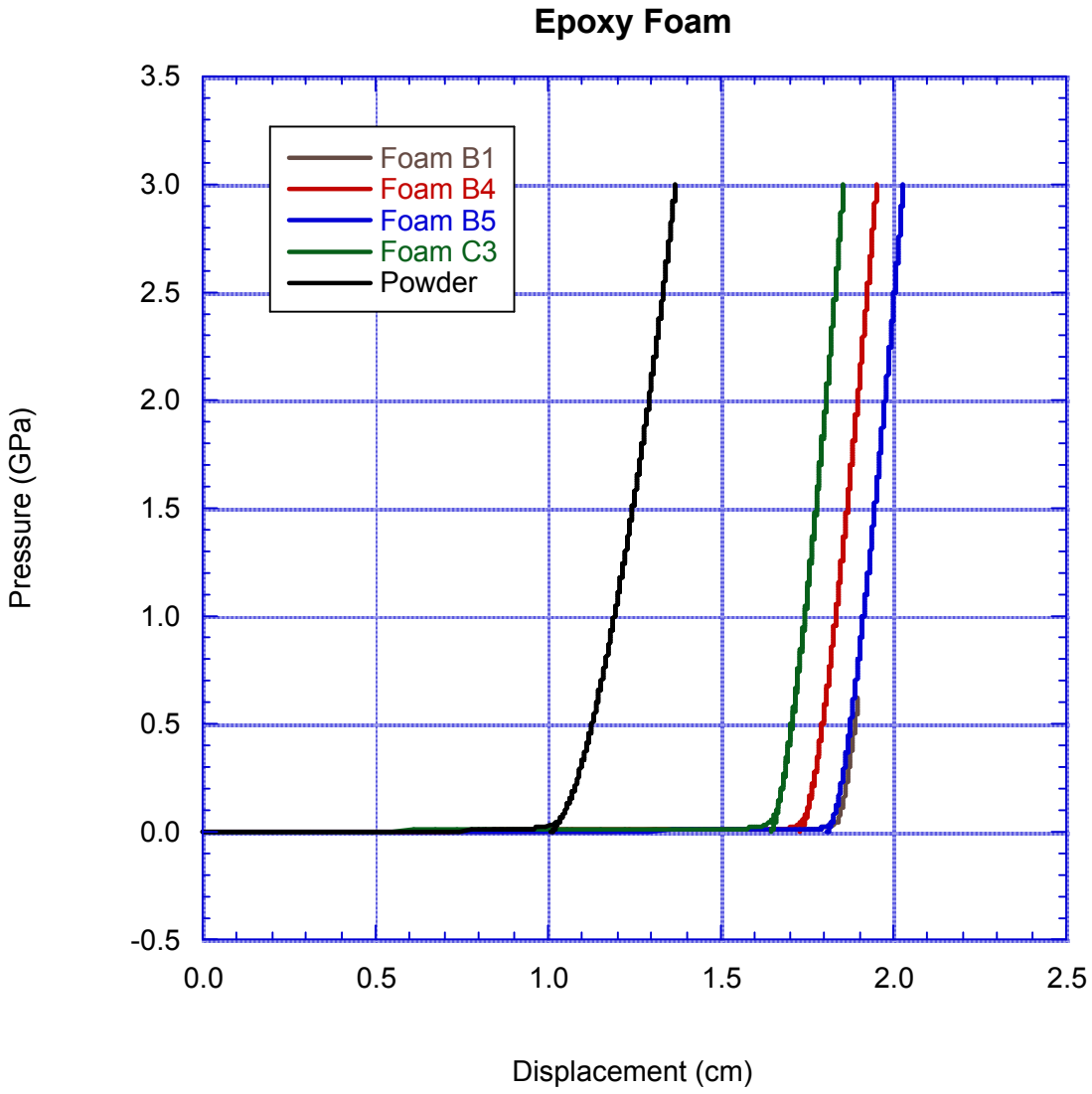

Fig. 14. Pressure vs. displacement curves for epoxy foam specimens and one specimen of crushed foam powder.

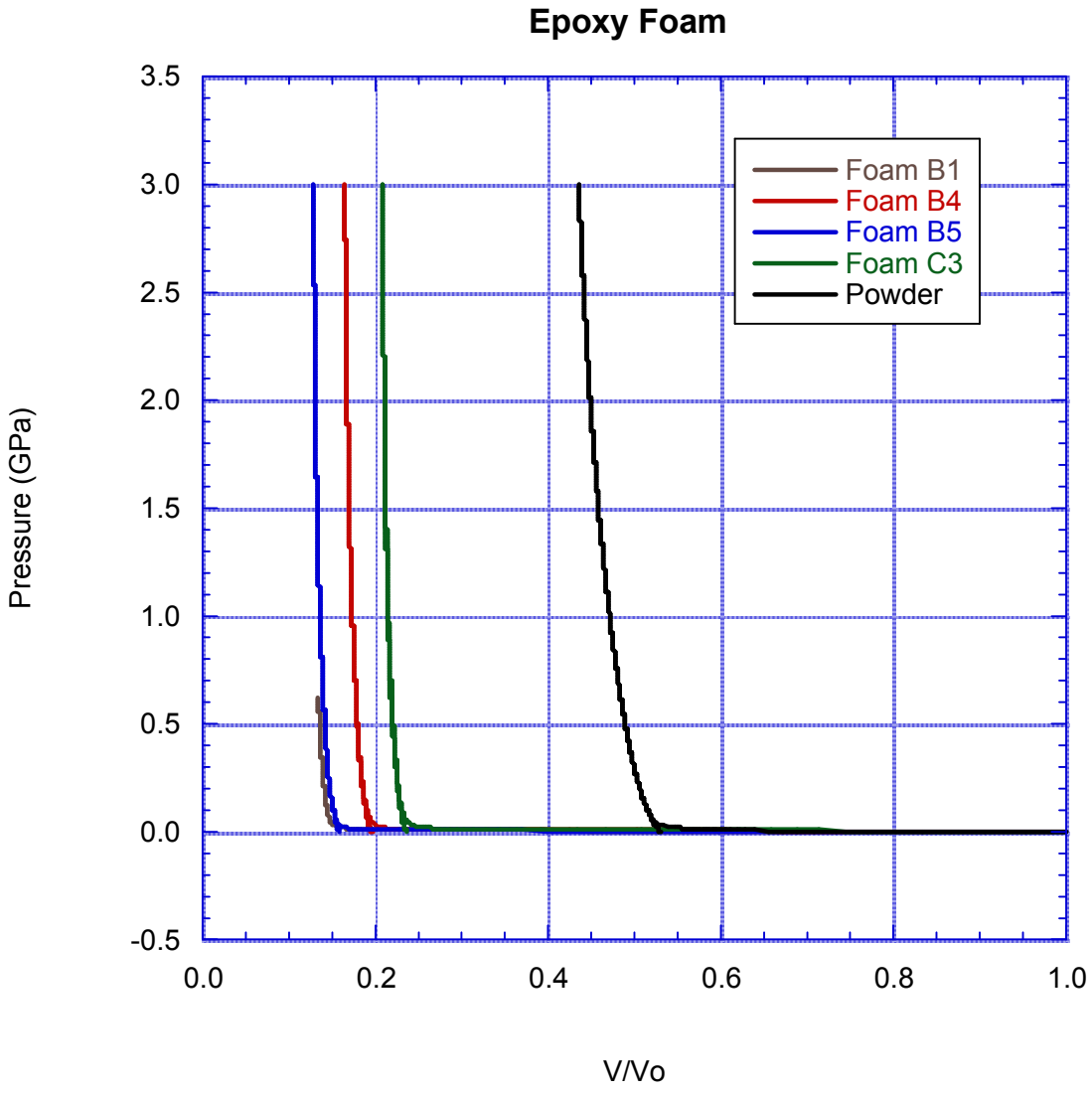

Fig. 15. Pressure-volume curves for epoxy foam and crushed foam powder. The test for Foam B1 terminated at 0.62 GPa.

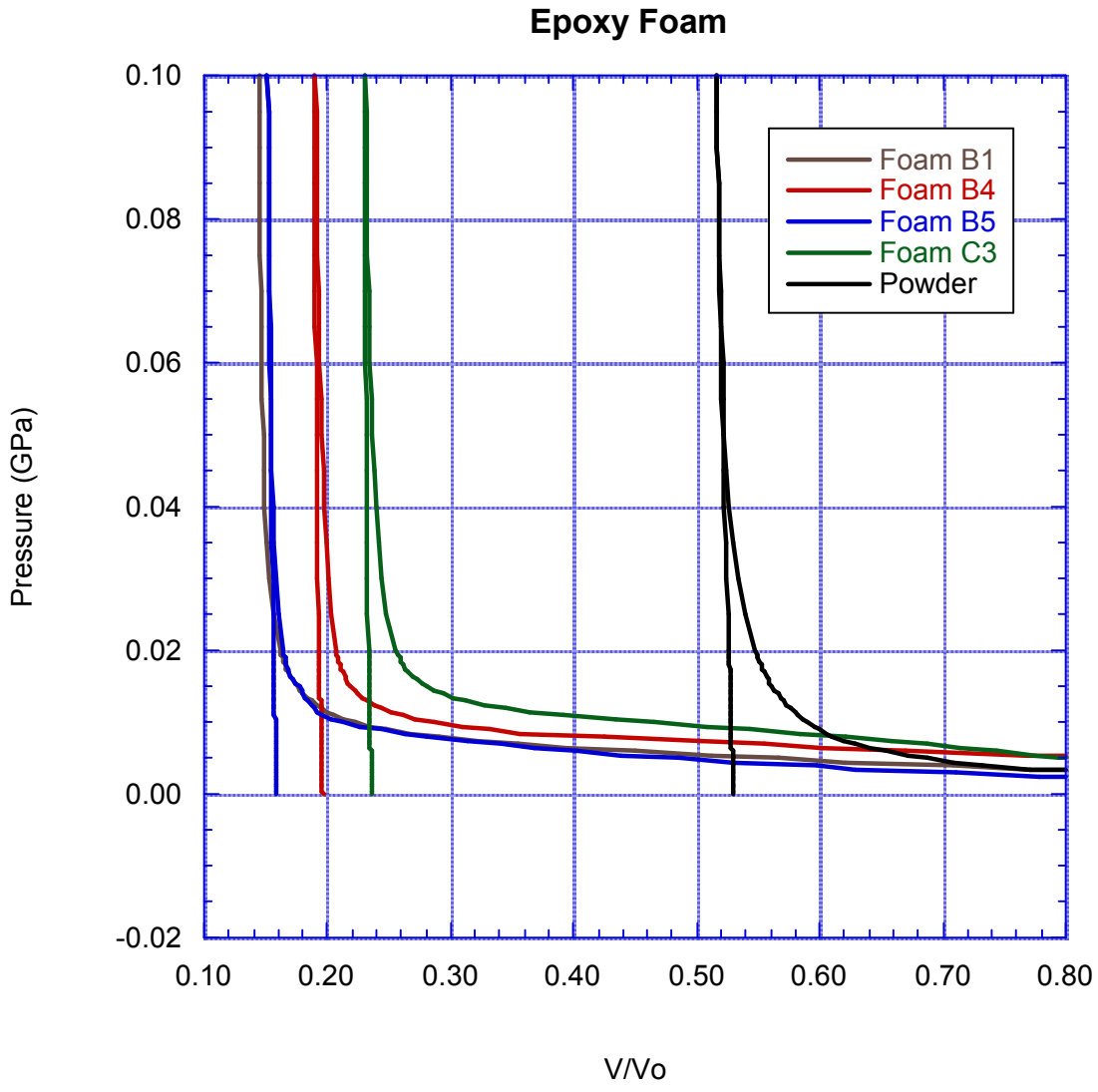

Fig. 16. Pressure-volume curves for epoxy foam and crushed foam powder to 0.1 GPa. The foam P-V curves steepen sharply at about 0.02 GPa. Initial foam porosities ranged from 79% to 82% and the initial powder porosity was about 45%. The pressure-volume curves indicate that nearly all porosity is removed by 0.05 GPa.

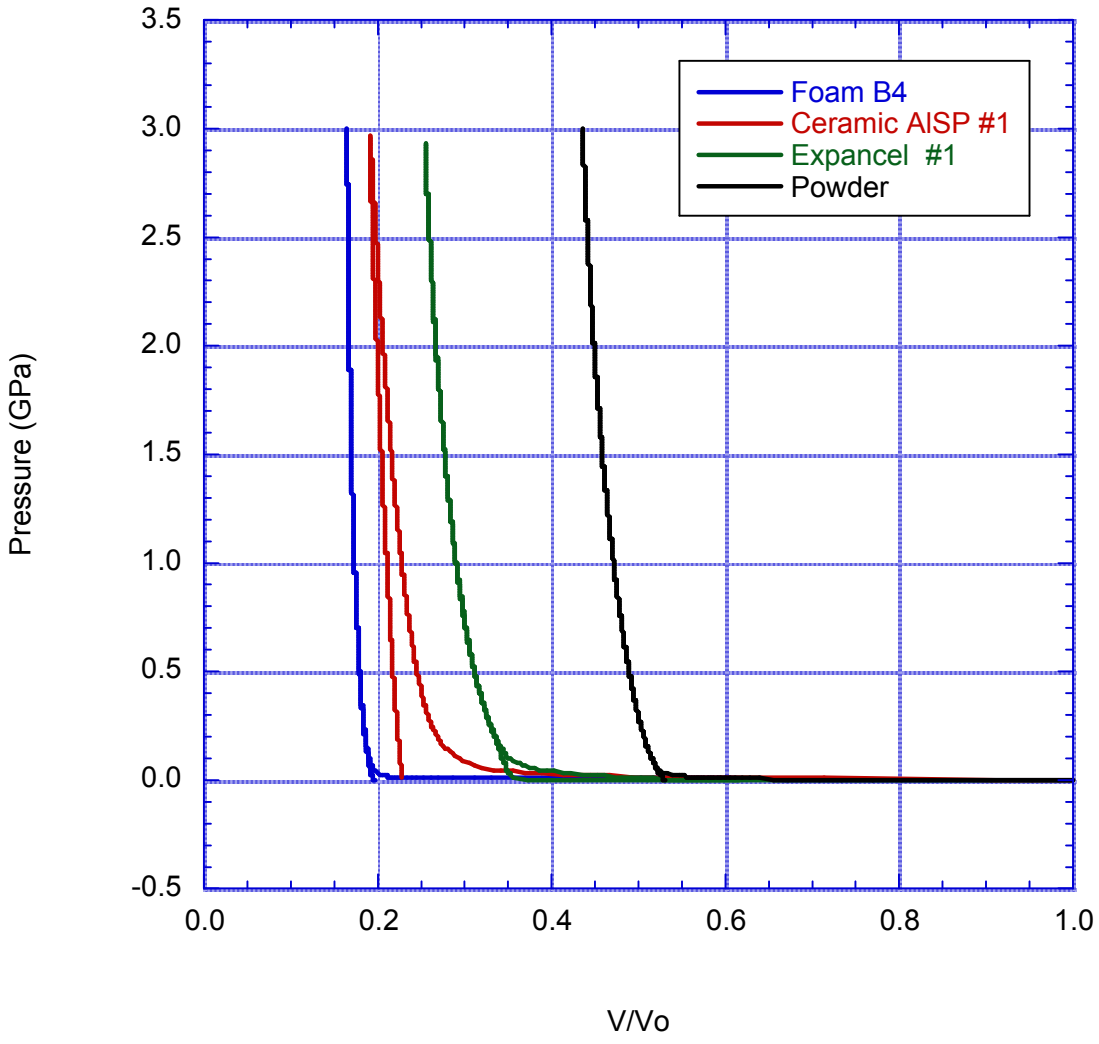

Fig. 17. Pressure-volume curves for four materials. The ceramic microsphere data are from Carlson et al. (2005). On loading, all of these materials undergo dramatic volume reductions at low pressure. On unloading, the foam and Expancel materials show more volume recovery than the brittle ceramic microspheres.

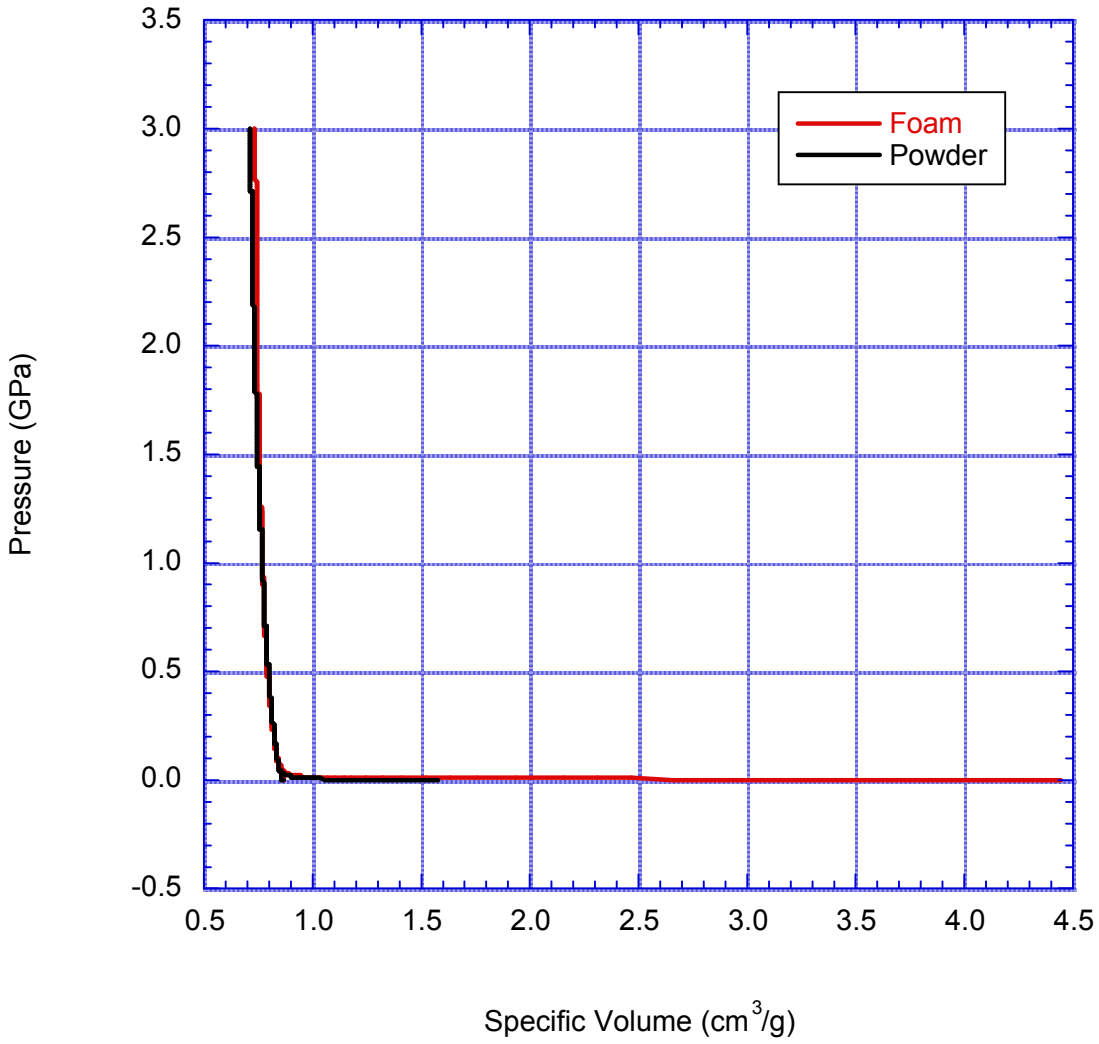

Fig. 18. Pressure vs. specific volume for "mean" foam and crushed foam powder. The "mean" foam was obtained by averaging the B4, B5 and C3 volume changes at each pressure. Although the initial specific volumes differ greatly, the curves match rather well after most of the initial foam porosity has been destroyed.

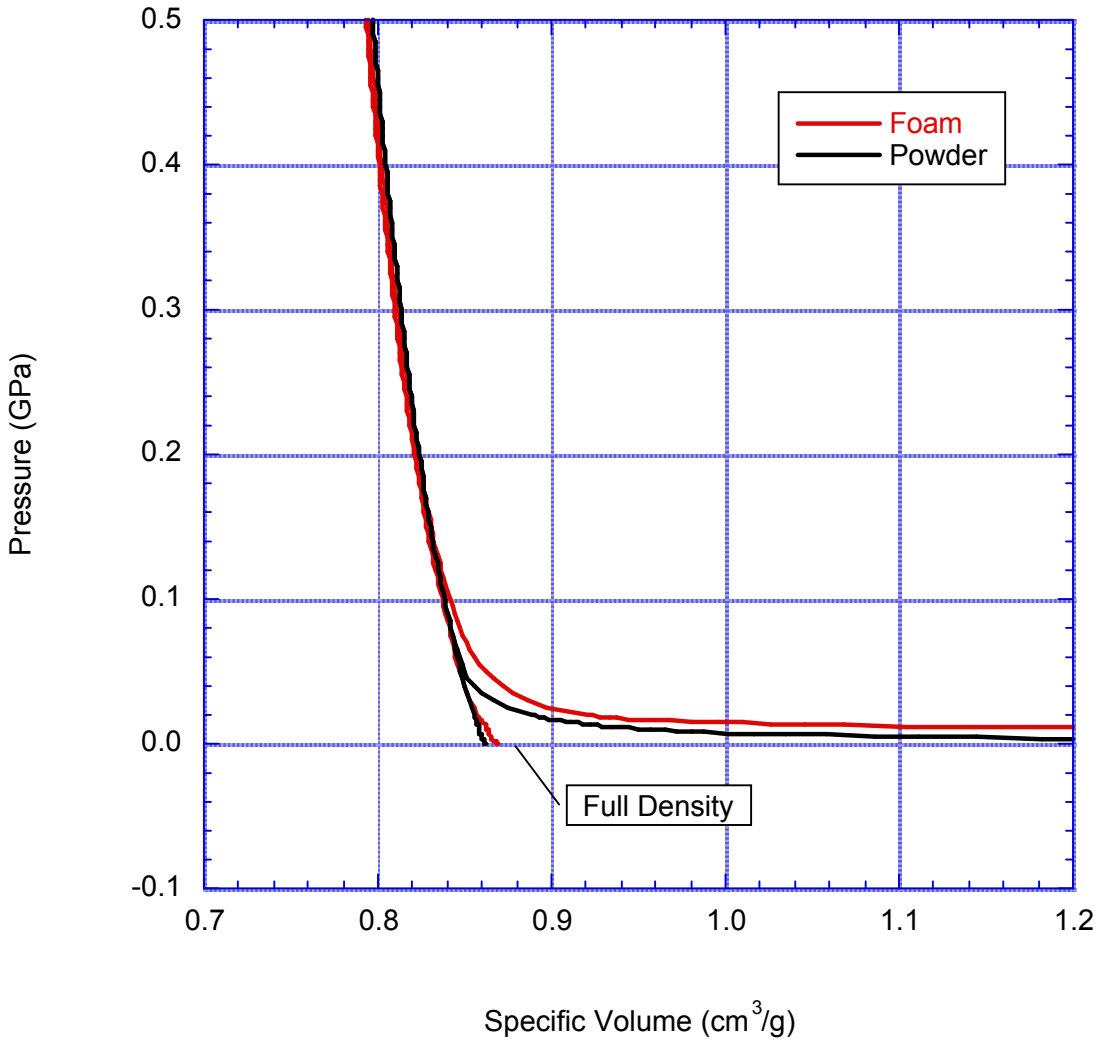

Fig. 19. Pressure vs. specific volume for "mean" foam and crushed foam powder. The scales have been expanded for clarity. The foam stiffens dramatically near full densification on loading and remains near full densification on unloading.

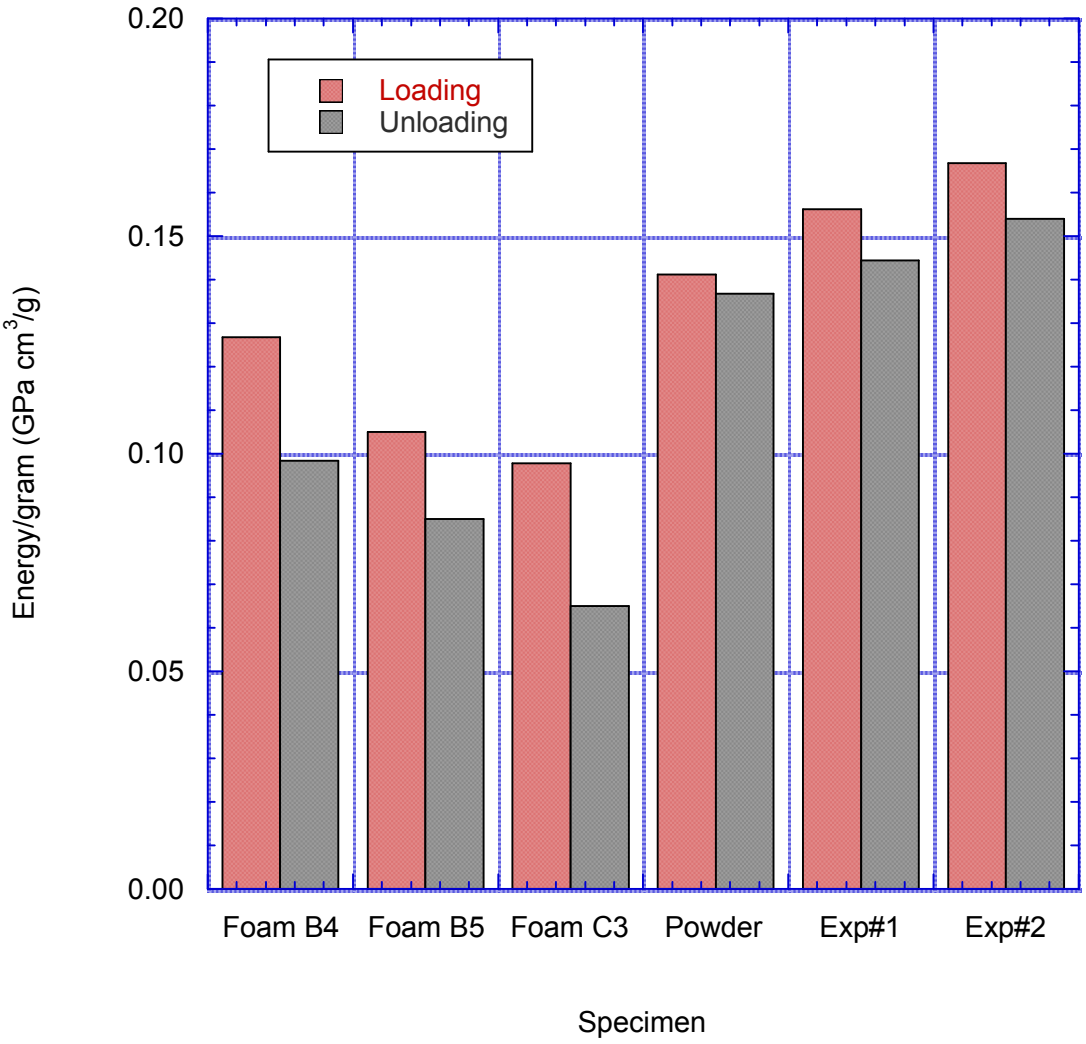

Fig. 20. Energy expended per gram in loading to 3 GPa (pink columns) and energy recovered per gram upon unloading (gray columns).

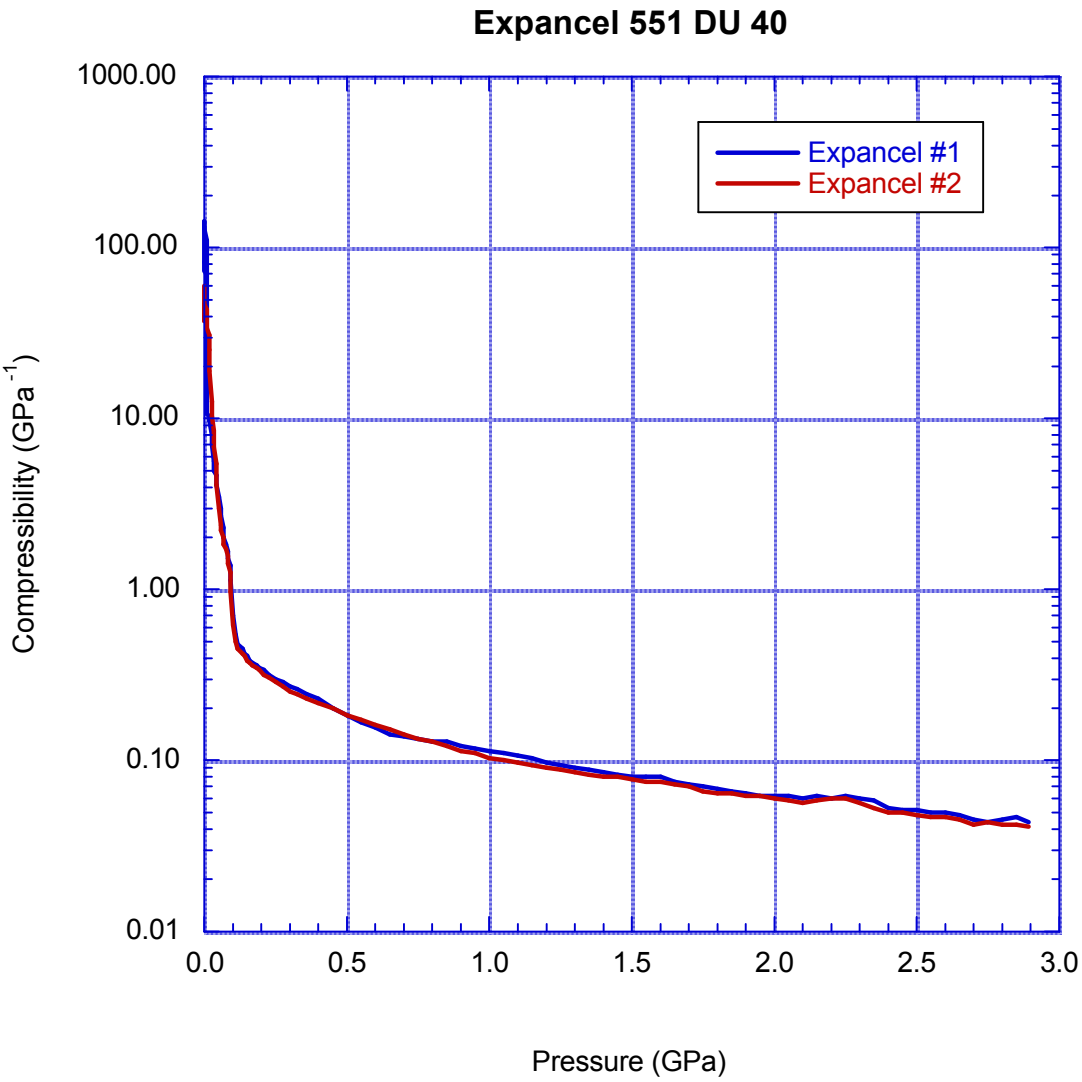

Fig. 21. Expancel compressibility.

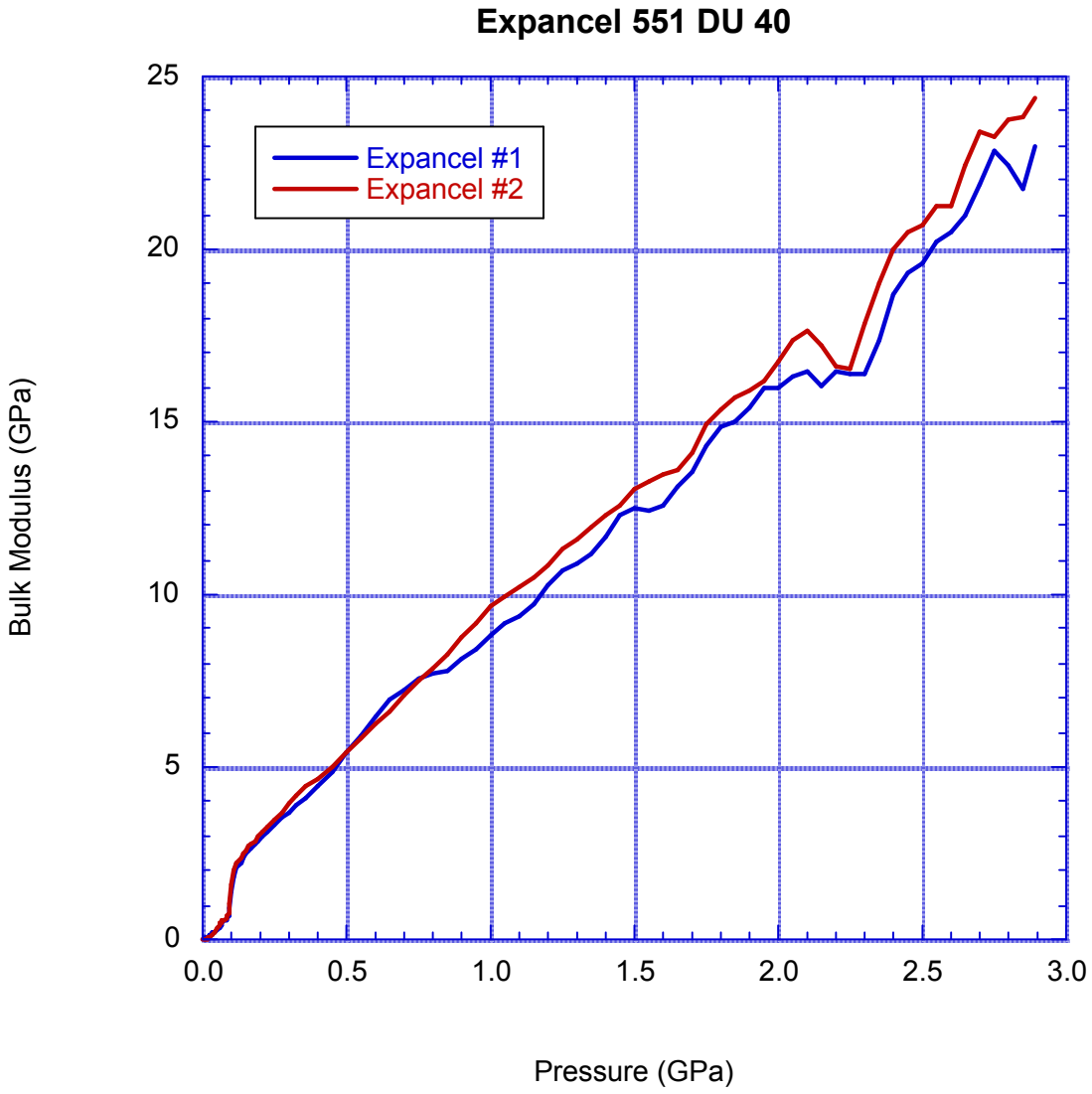

Fig. 22. Tangent bulk modulus for Expancel microspheres. The bulk modulus rises rapidly below 0.1 GPa, and increases linearly with pressure above 0.1 GPa. A linear increase in bulk modulus with pressure is often observed for liquids (Hayward, 1974).

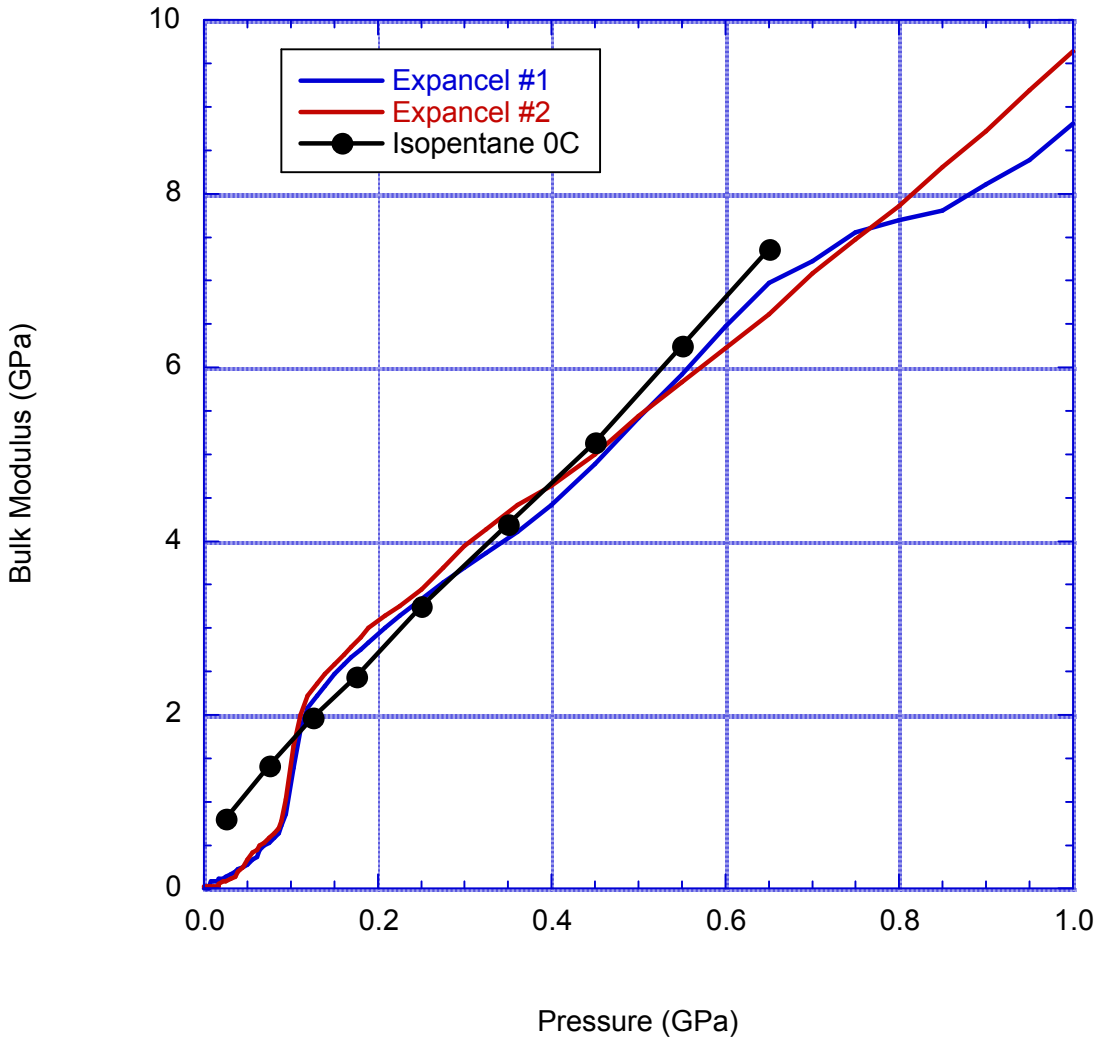

Fig. 23. Bulk modulus of Expancel at room temperature and isopentane at 0°C. The isopentane data are from Bridgman (1964c). Below 0.1 GPa the Expancel microspheres are more compliant than isopentane due to air/gas in the pore space. After the porosity is removed, the Expancel bulk modulus closely matches that of isopentane.

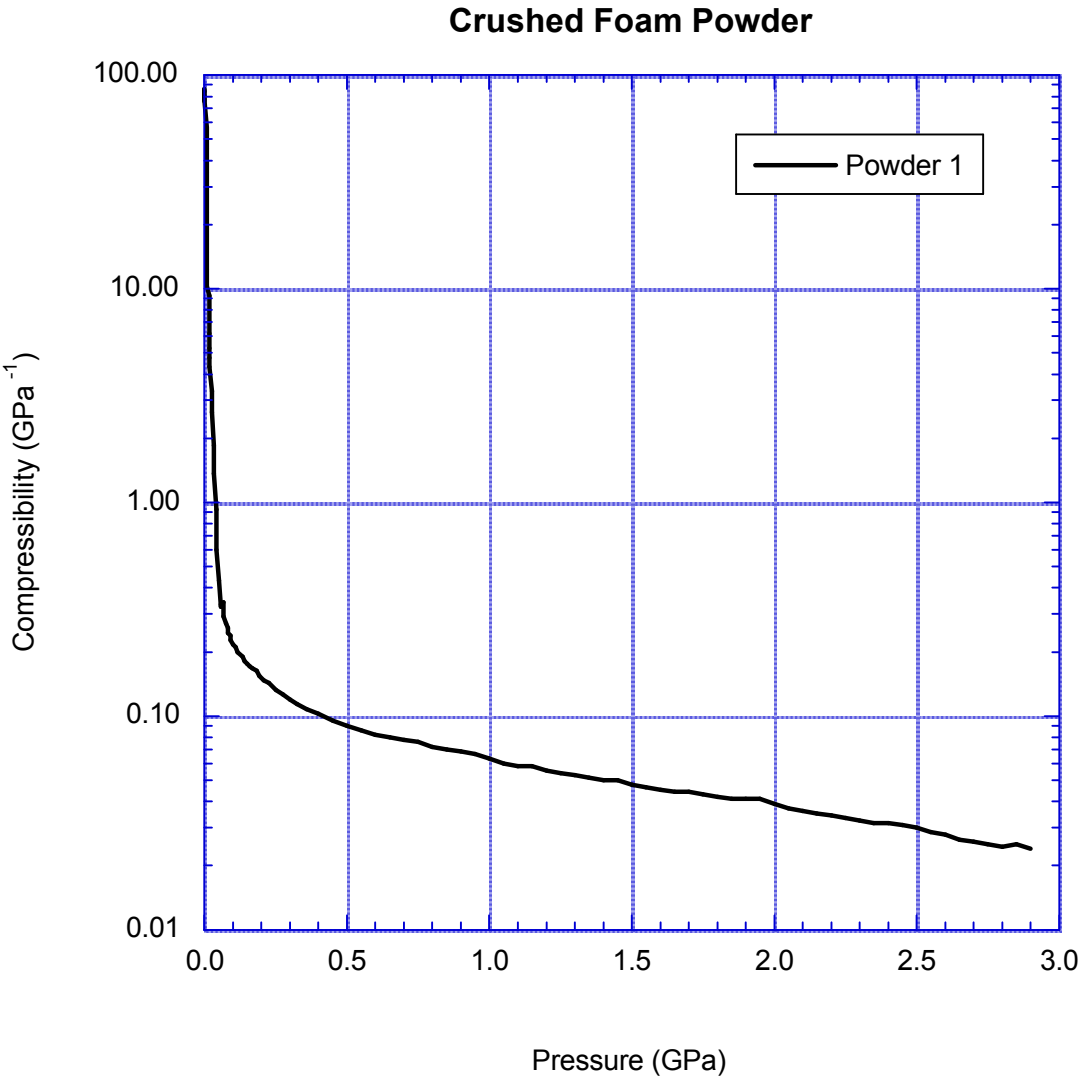

Fig. 24. Compressibility of crushed foam powder.

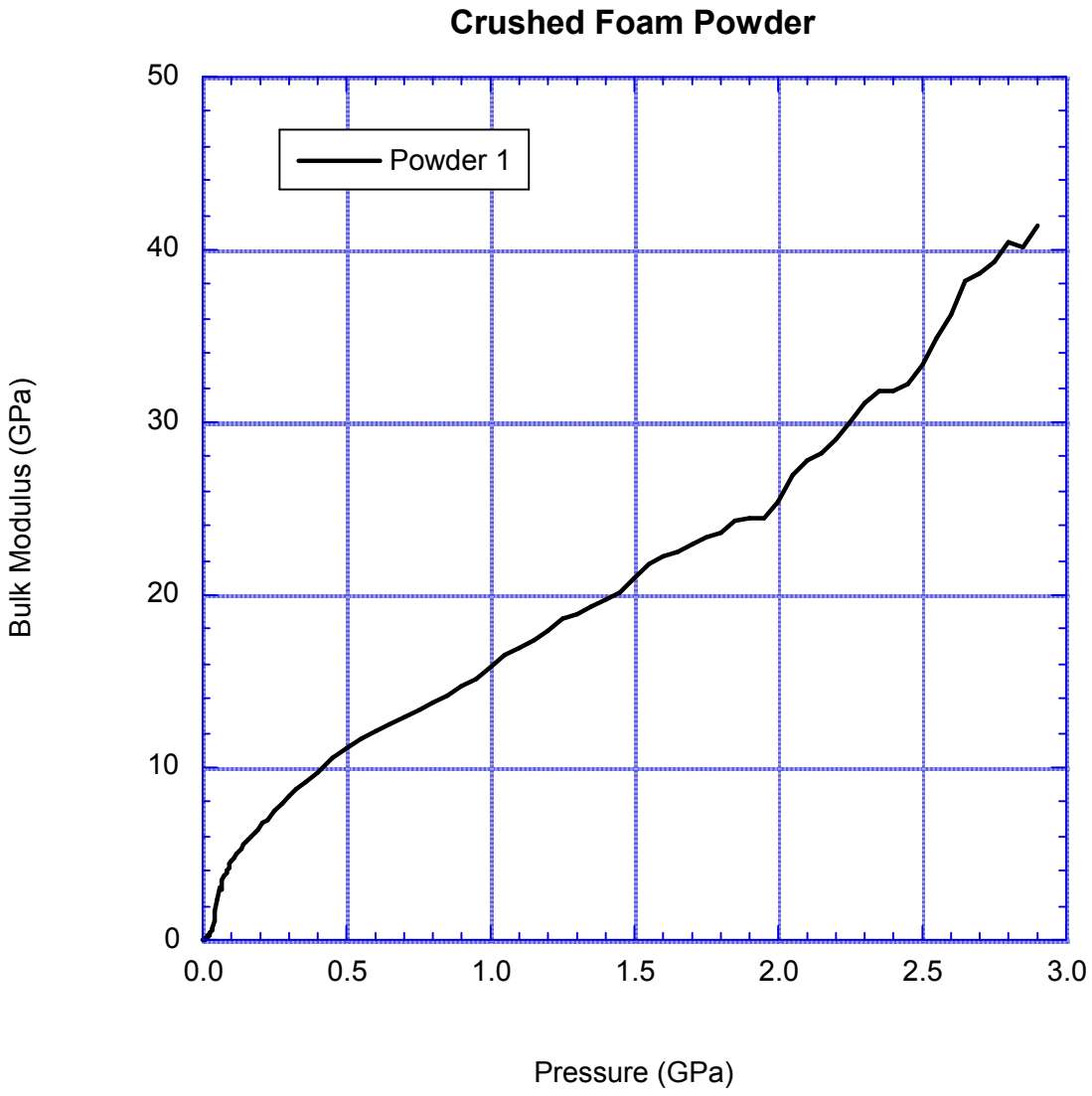

Fig. 25. Tangent bulk modulus of crushed foam powder.

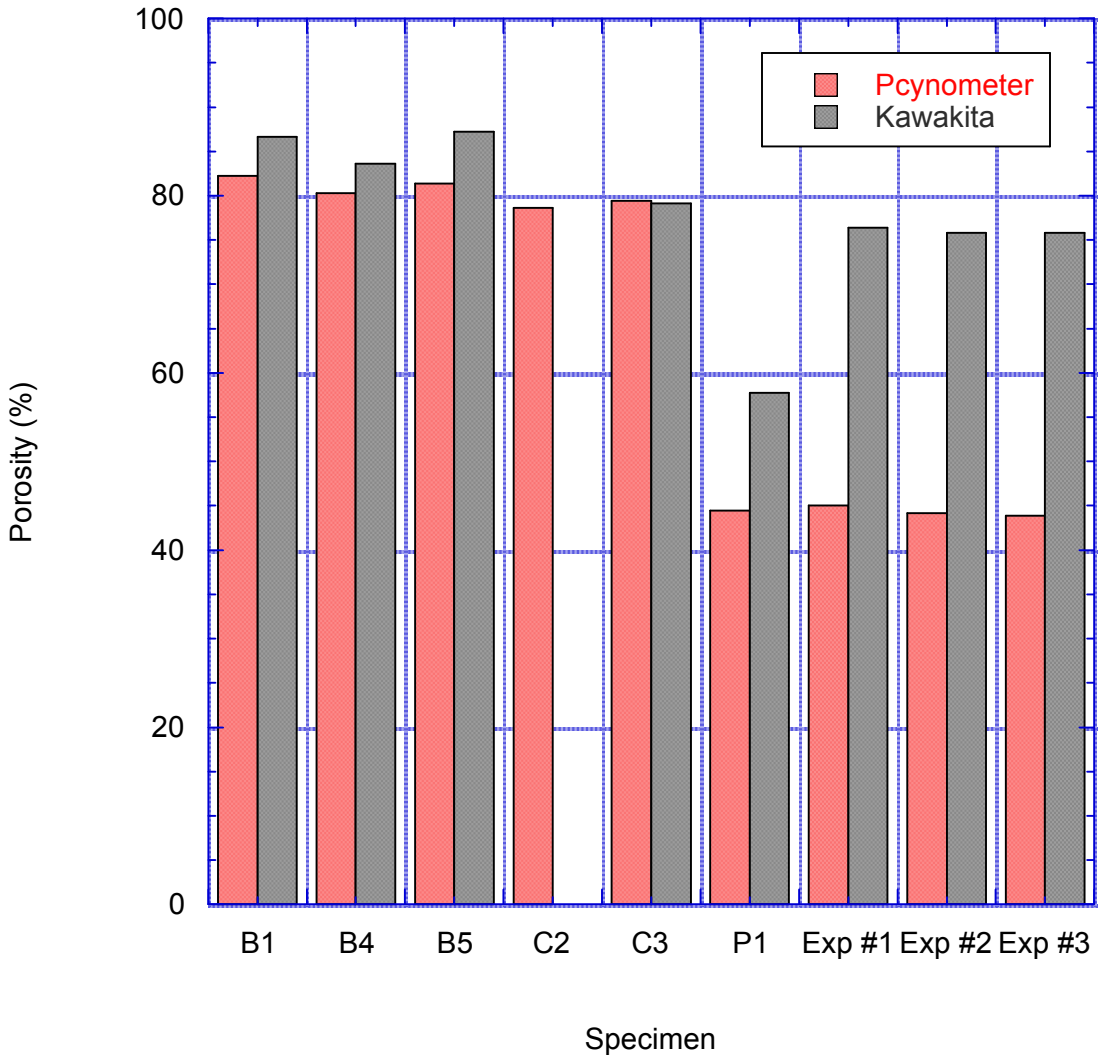

Fig. 26. Initial porosity for epoxy foam (B1 – C3), crushed foam powder (P1), and Expancel microsphere specimens. The pink columns are porosities calculated from pycnometer measurements of powder volumes. The gray columns are porosities calculated from Kawakita model fits to the pressure-volume data. The pycnometer measurements miss much of the Expancel porosity if the Expancel shells are impermeable to helium.

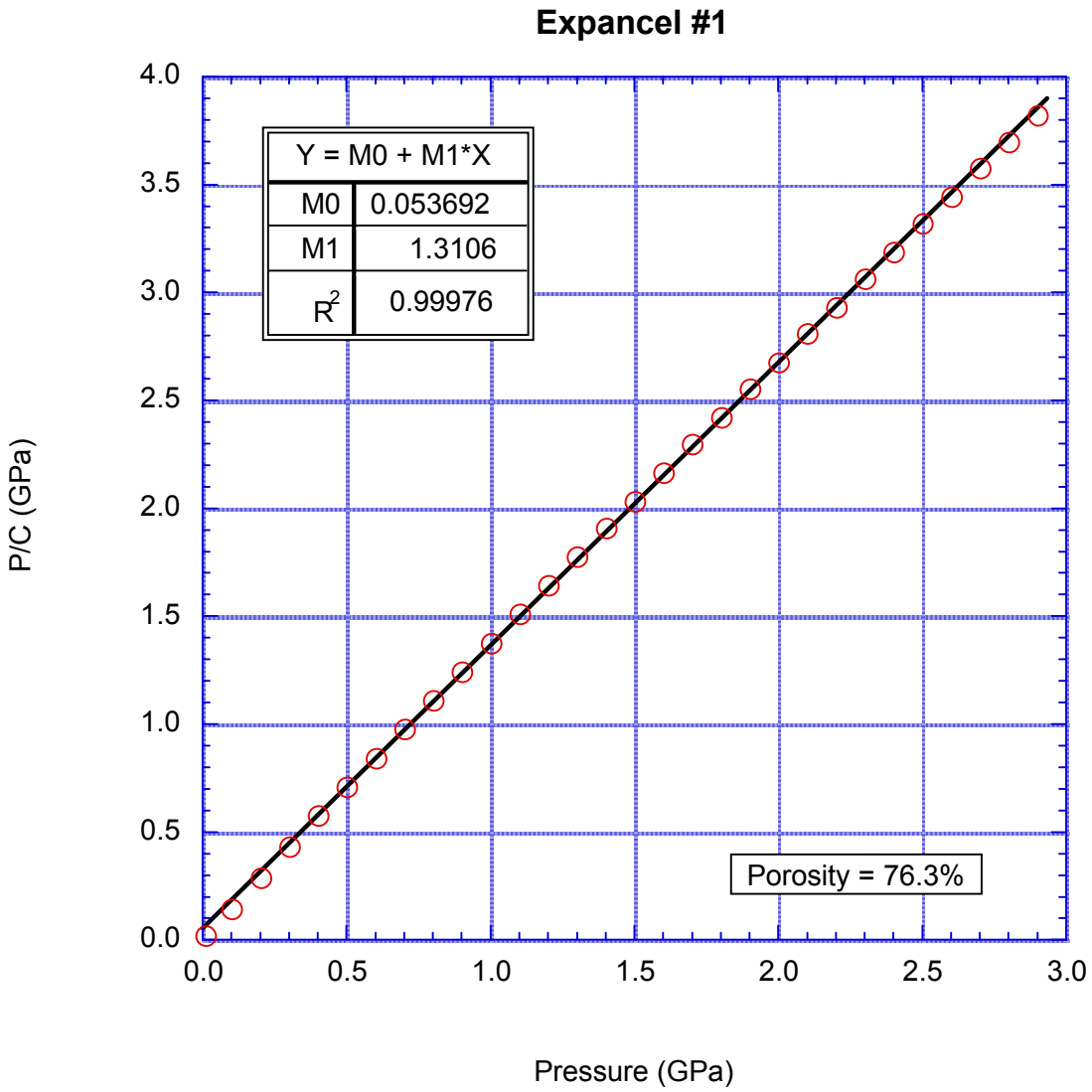

Fig. 27. Kawakita model fit to Expancel #1 pressure-volume data. Only 5% of the data are plotted for clarity. The regression slope of 1.3106 corresponds to an initial specimen porosity of 76%. Since the pycnometer measurements indicate an "exterior" porosity of 45%, the other 31% represents the void space inside of the hollow microspheres.

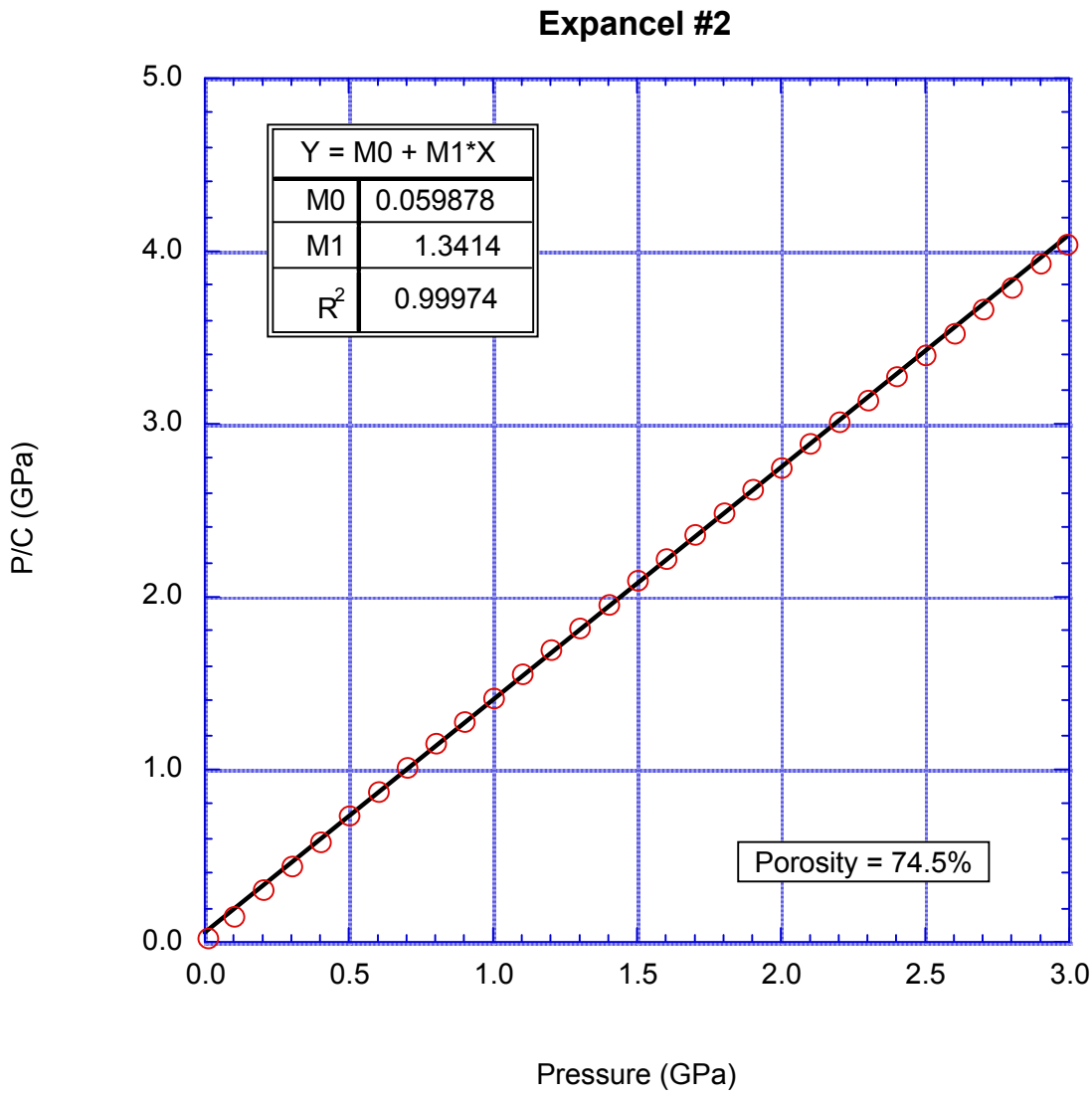

Fig. 28. Kawakita model fit to Expancel #2 data. Only 5% of the data are plotted for clarity. The regression slope of 1.3414 corresponds to an initial specimen porosity of 75%, only slightly below the previous specimen. Since the pycnometer measurements indicate an "exterior" porosity of 44%, the other 31% represents "interior" porosity in good agreement with the previous specimen.

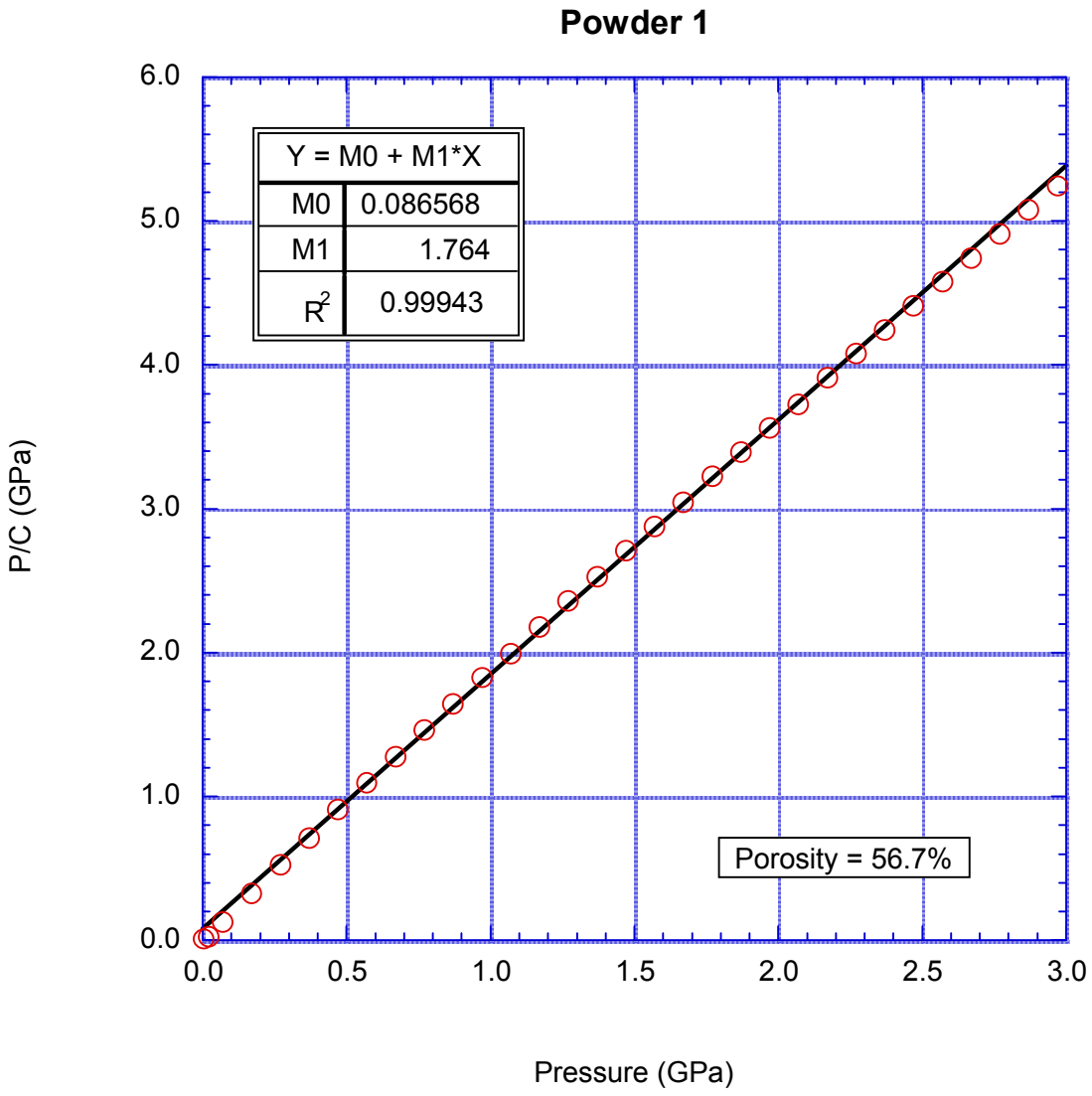

Fig. 29. Kawakita model fit to crushed foam powder. Only 5% of the data are plotted for clarity. The regression slope of 1.764 corresponds to an initial specimen porosity of 57%, somewhat higher than the 45% porosity found from the pycnometer data.

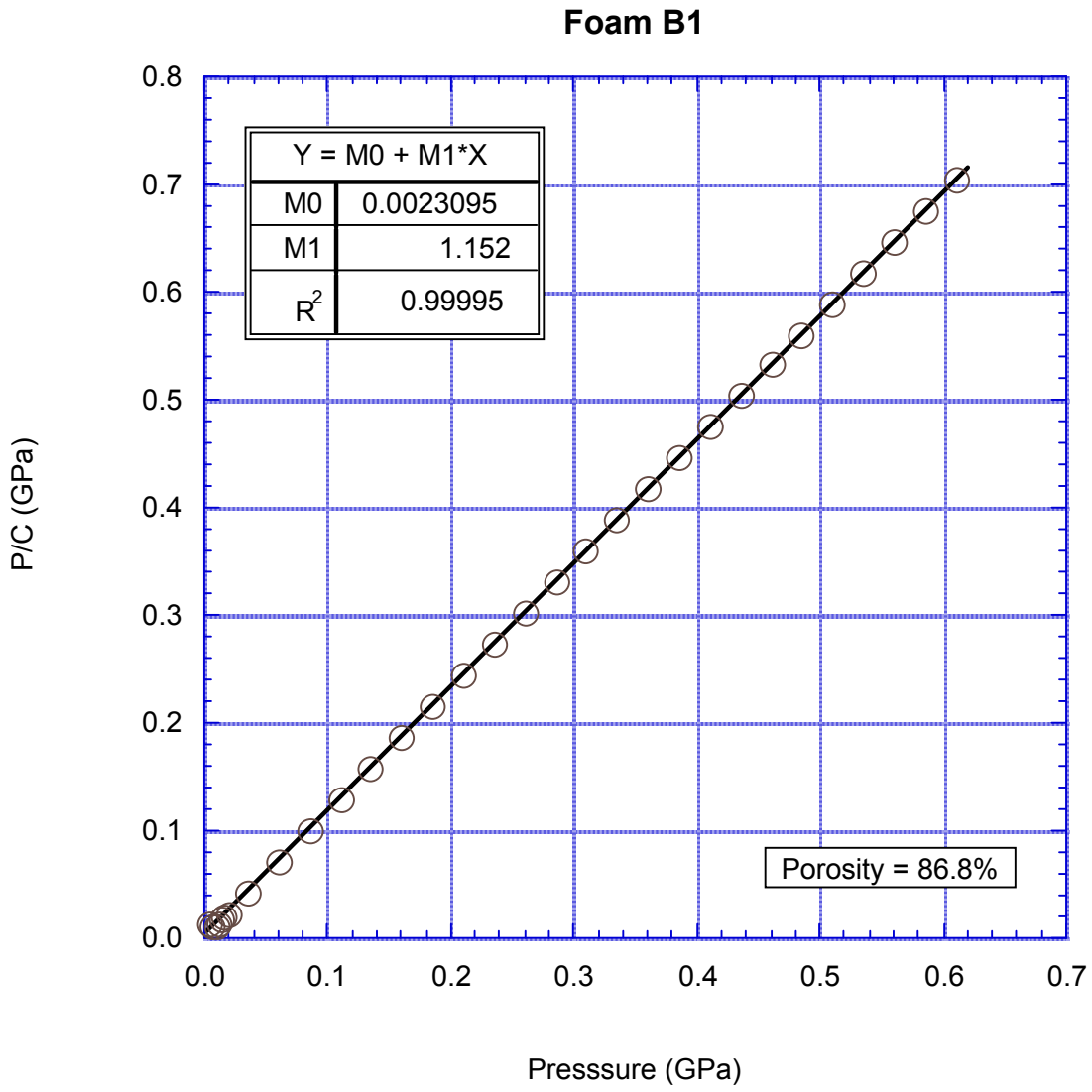

Fig. 30. Kawakita model fit to foam B1. Only 20% of the data are plotted for clarity. The regression slope of 1.152 corresponds to an initial specimen porosity of 86.8%, higher than the 82% porosity found from the pycnometer data.

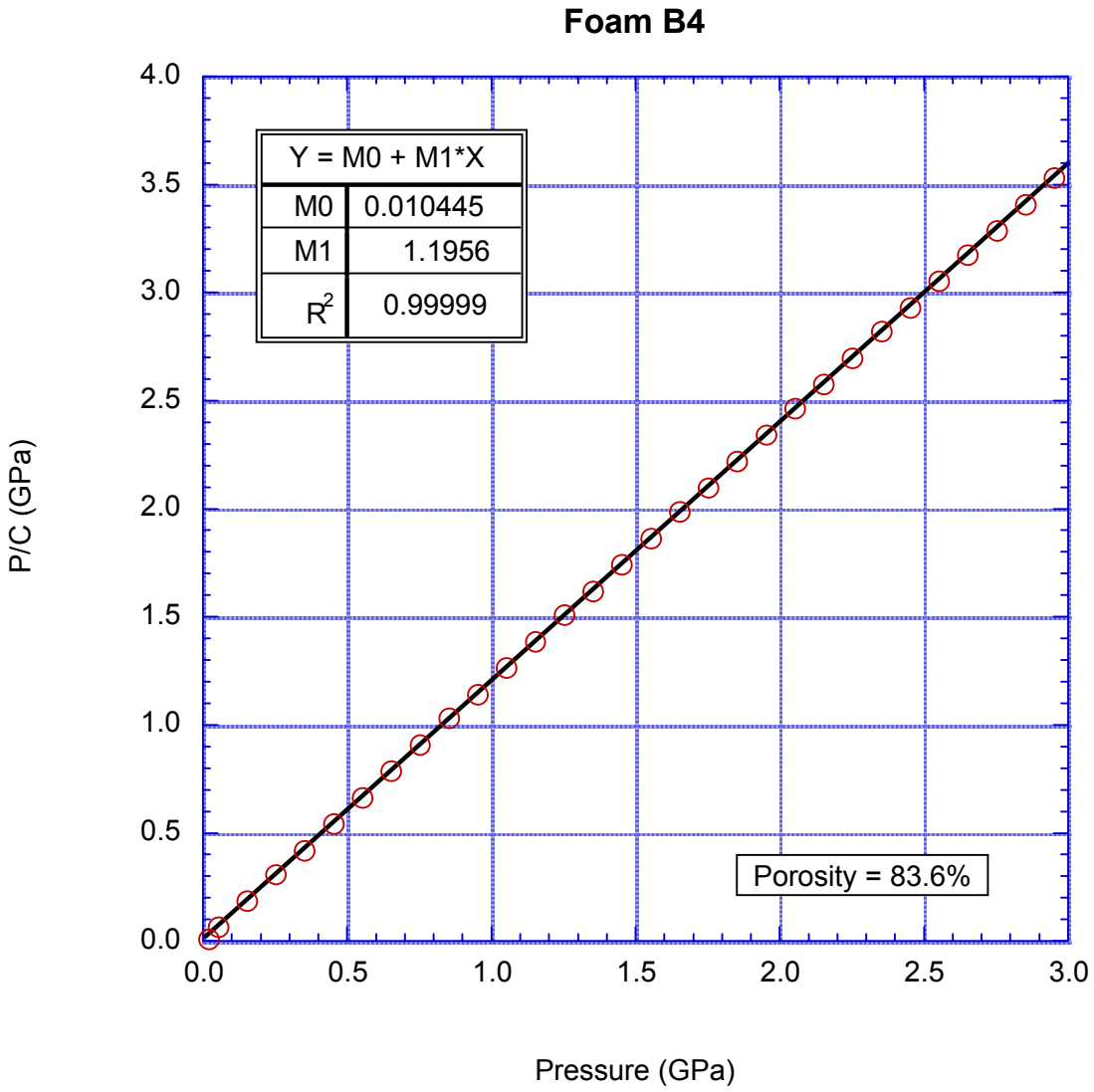

Fig. 31. Kawakita model fit to foam B4. Only 5% of the data are plotted for clarity. The regression slope of 1.1956 corresponds to an initial specimen porosity of 84%, somewhat higher than the 80% porosity found from the pycnometer data.

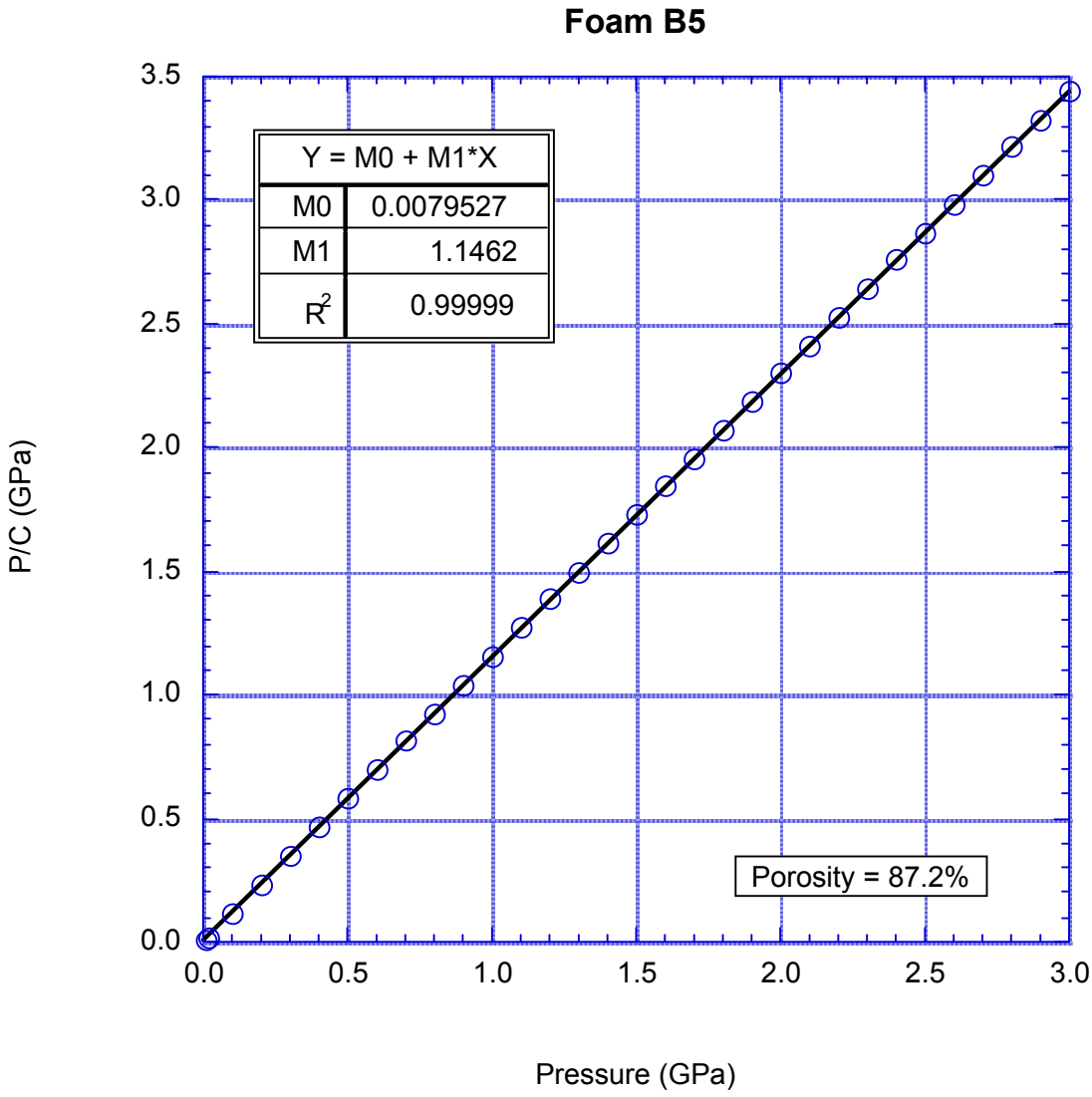

Fig. 32. Kawakita model fit to foam B5. Only 5% of the data are plotted for clarity. The regression slope of 1.1462 corresponds to an initial specimen porosity of 87%, clearly higher than the 81% porosity found from the pycnometer data.

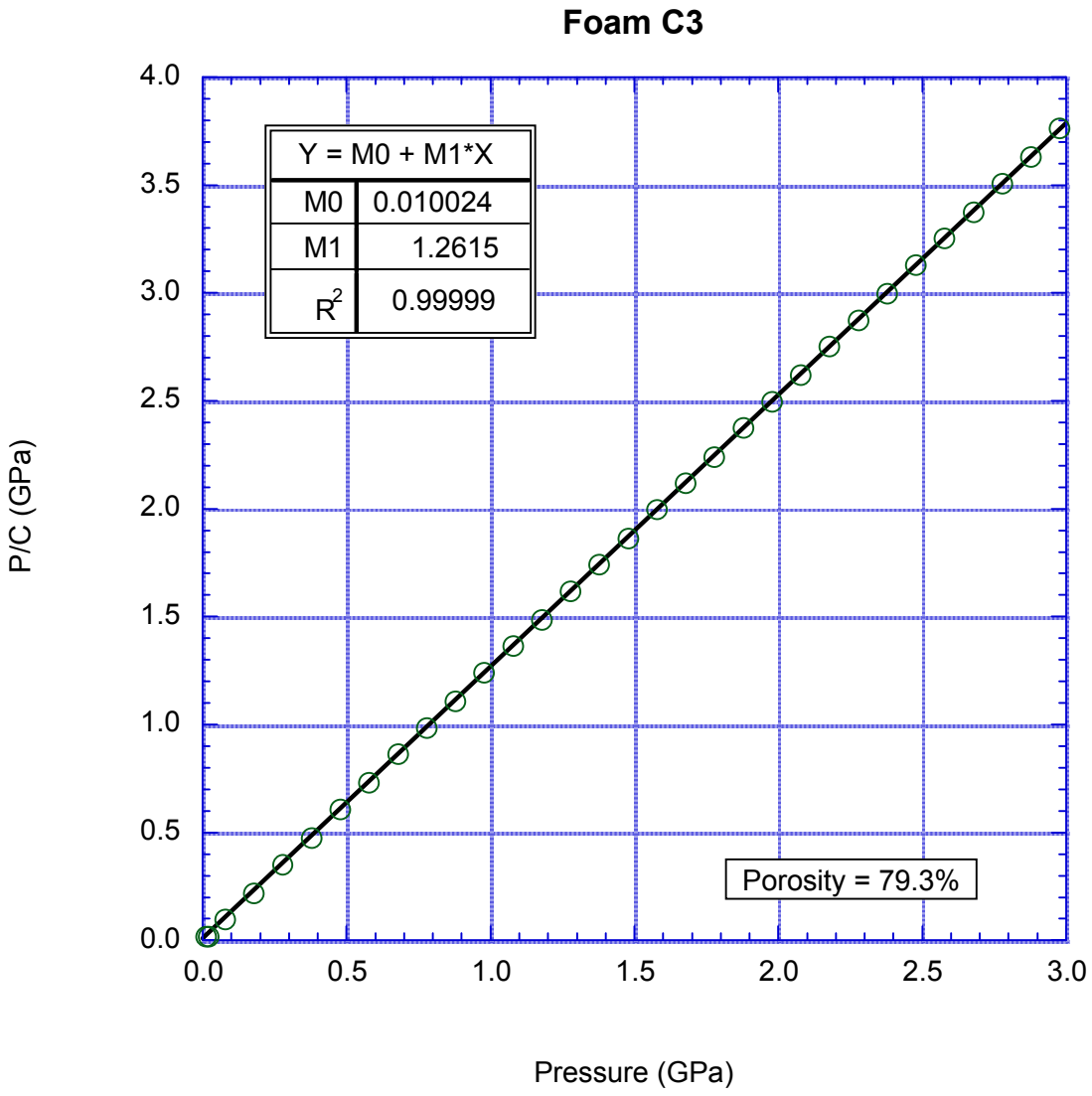

Fig. 33. Kawakita model fit to foam C3. Only 5% of the data are plotted for clarity. The regression slope of 1.2615 corresponds to an initial specimen porosity of 79.3%, in excellent agreement with 78.6% porosity found from the pycnometer data.